Departmental Report Clearance Letter

Department of Civil Engineering

This signed clearance letter must be on file in ECJ 4.2
prior to the first day of finals in order for you
to be cleared for graduation.
In addition, your advisor must assign you a
final grade.

Date: August 4, 1995

This will certify that Gordon B. Fox has completed

a Departmental Report and that it has been accepted by the student's committee.

Signed:

Richard E. Klingner, PhD.
Supervising Professor

Richard W. Furlong, PhD.
Reader

Graduate Advisor

USE OF INJECTION GROUTING / GROUTED METAL TIES TO IMPROVE SEISMIC RETROFITTING OF UNREINFORCED MASONRY (URM) BUILDINGS

by

Gordon B. Fox

Departmental Report

Presented to the Faculty of the Department of Structural Engineering of
the University of Texas at Austin
in Partial Fulfillment
of the Requirements
for the degree of

Master of Science in Engineering

The University of Texas at Austin
August 1995

ACKNOWLEDGEMENTS

The research project for which this report was conceived is a team effort by Professor Richard E. Klingner, Graduate Research Assistant Brian Harris and the author. The assistance of Professor Klingner in the use the SAP90 Structural Analysis Program software is especially appreciated, as well as his technical advice in simplifying the computer model while maintaining the validity of its analytic representations. Also, special thanks go to Rina Fox, and the author's parents, Gordon and Christine for their support and encouragement during this challenging year.

TABLE OF CONTENTS

LIST OF FIGURES

CHAPTER 1: INTRODUCTION

1.1. General

Unreinforced masonry (URM) structures have performed poorly in past earthquakes and are a life-safety hazard in active seismic areas. Major earthquakes in California such as the 1906 San Francisco and 1933 Long Beach events caused many deaths in and around URM structures from collapses within the building and debris falling outside the building. After the Long Beach tragedy in 1933 when many URM schools collapsed on the children inside, masonry construction was outlawed in public buildings in California and all but abandoned until the mid 1940's when updated building codes for seismic performance of masonry helped bring back the use of masonry as a construction material (The Masonry Society (TMS) 1994). Today, reinforced masonry technology has advanced such that modern masonry structures perform at least as well in earthquakes as their steel and reinforced concrete counterparts.

This report considers only URM structures of the type built in southern California prior to the 1933 Long Beach earthquake. In general, these were bearing wall structures with wall thicknesses of 12 inches for low-rise buildings (one to three stories), increasing to 16 inches or more at greater heights. Parapet walls were either the same thickness as the bearing wall or one wythe thinner (Green 1993). These structures were designed primarily for gravity loads, and therefore lack the ductility and toughness required to withstand repeated load reversals caused by severe wall and diaphragm oscillations during earthquakes. As a result, URM buildings can experience dramatic failures due to lack of anchorage between diaphragms and walls, failure of anchors when present, in-plane shear failure of masonry, out-of-plane tensile bending or buckling failure of walls, failures due to combined in-plane and out-of-plane effects, and diaphragm-related failures (Bruneau 1994).

During strong earthquakes, anchorage failures often occur in masonry structures where floor and roof diaphragms rest on masonry corbels or joist pocket connections, with only the friction from the diaphragm weight to resist lateral forces. Large wall deflections cause the diaphragm to pull off the support and collapse onto the level below. Such failures can lead to catastrophic building collapses. Even when anchors are present, failures can occur when the metal anchor breaks or the adjacent masonry crumbles (Bruneau 1994).

In-plane shear failures of URM buildings are evidenced by diagonal one-way or two-way (x-shaped) cracking of URM piers caused by lateral forces during earthquakes. Minor or hair line cracking does not normally compromise the gravity load carrying capacity of the wall. However, wide x-cracking of piers is indicative of a structural failure of the pier in shear. Figure 1.1 below is a representation of this failure mode, showing a URM pier that is no longer stable after shear cracking.

Out-of-plane failures occur as a result of deflections of flexible diaphragms pushing outward on walls, or simply by excessive wall deflections leading to instability and buckling. Improperly bonded multi-wythe walls can behave as several independent walls during earthquakes, causing separation of the wythes and subsequent wall failure. The exterior wythe fails first due to lack of support from adjacent structural elements. These effects are aggravated by large height-to-thickness ratios of walls.

Combined in-plane and out-of-plane failures occur when bi-directional earthquake forces cause a combination of the failures described above. For example, as in-plane shear cracking occurs, triangular cantilever wedges are produced, reducing the out-of-plane strength of the wall, which can lead to collapse. Also, pounding of adjacent structures during earthquakes can cause these failures. Refer to Figure 1.1.

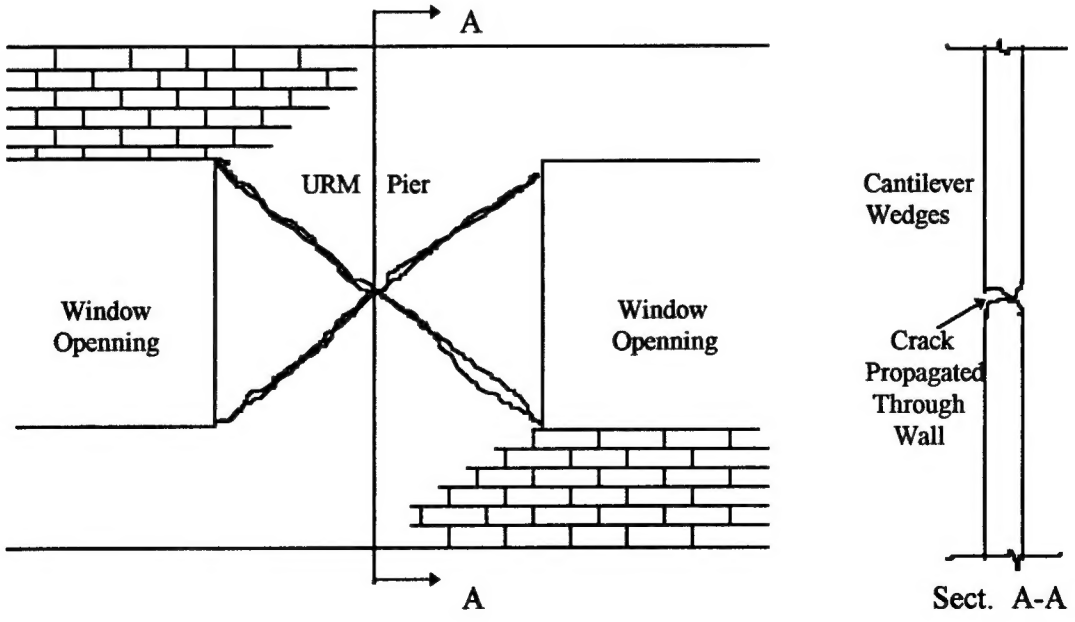

Figure 1.1: X-Cracking of URM Pier with loss of out-of-plane stability

Finally, diaphragm-related failures result when deflection of flexible diaphragms against walls causes instability and buckling, or when inadequate shear resistance of rigid diaphragms causes them to slip and crack the masonry walls at the corners (Bruneau 1994). There can also be combinations of the above effects.

During the 1989 Loma Prieta, California earthquake, numerous parapet and wall collapses occurred due to out-of-plane failures. The taller parapets on the fronts of URM buildings acted as cantilevers, failing due to tensile bending forces caused by out-of-plane effects during the earthquake. In one instance, collapsing parapets and walls fell on people in the street, causing five deaths. Also, parapets installed to slow the spread of fire between structures, collapsed through the roof of lower adjacent buildings, resulting in several deaths (Green 1993).

In 1981, Division 68 of the Los Angeles Building Code was introduced to provide a minimum standard for life-safety protection in URM bearing wall structures built, under construction, or permitted prior to October 6, 1933. Division 68 was updated in 1985 as Division 88, which added requirements for testing and strengthening of mortar joints to meet minimum shear strength requirements. Division 88 required that URM walls be positively anchored to floor and roof diaphragms, and that parapet walls be braced or removed. The ordinance also added parapet height limitations and a requirement for continuous inspection of retrofitting work (TMS 1994).

Unfortunately, Division 88 has not solved all of the URM problems in Los Angeles. During the January 17, 1994 Northridge, California earthquake, retrofitted structures generally behaved much better than did unretrofitted buildings. However, even some of the retrofitted structures sustained significant damage. Typical failure modes were punching shear failures of the masonry at brace points, and failures due to out-of-plane action and instability of walls. In addition, unretrofitted structures outside the city limits northwest of the epicenter experienced major damage, and continue to be a hazard.

1.2. Objectives and Scope of Project

A National Science Foundation (NSF) sponsored research project at the University of Texas at Austin, under the supervision of Professor Richard E. Klingner, is investigating methods for improving the performance of URM parapets retrofitted in accordance with Division 88. Several techniques will be studied, including injection grouting of masonry cracks and the drilling and

insertion of metal ties to strengthen the bond between existing wythes. The experimental phase of the project will include dynamic testing of four parapet specimens. Three will be braced per Division 88 and built with one or both of the above retrofitting improvements. The fourth will be braced per Division 88, but will have no further improvements. A Master's Thesis will be published separately reporting the overall project results.

The objectives and scope of the research project are as follows:

1. To review and report current Division 88 requirements for URM retrofitting.
2. To review and report the current state of knowledge regarding grout for grout injection.
3. To set up a prototypical parapet testing facility in the laboratory and perform dynamic testing of four URM subassemblages, three with injection grouting and/or grouted metal ties and one baseline specimen braced per Division 88, but with no further improvements.
4. Based on the results of the testing, to recommend grout injection procedures to improve URM retrofitting measures prescribed by Division 88.

1.3. Objectives and Scope of Report

The objectives and scope of this report are as follows:

1. To introduce the project by discussing the January 17, 1994 Northridge, California earthquake which led to the inception of the research project.
2. To briefly discuss the modern history of URM construction and the various retrofitting technologies available.
3. To discuss the requirements set forth in Division 88 of the City of Los Angeles Building Code.

4. To set the framework for the experimental phase of the project by presenting the structural dynamic theory of the problem, and by calculating the response of a typical URM building at roof level to earthquake ground motions recorded during the Northridge earthquake.

5. To convert the calculated response to idealized programmable time histories of acceleration, velocity and displacement to aid in the design of the dynamic loading apparatus for the laboratory specimens.

CHAPTER 2: BACKGROUND

2.1. The Northridge Earthquake

At 4:31 a.m. on January 17, 1994, one of the few major earthquakes to directly affect a heavily populated urban area in the United States shook the city of Northridge, California, in the San Fernando Valley approximately 30 miles northwest of central Los Angeles. The earthquake had a moment magnitude of 6.7 and occurred on a previously unmapped thrust fault. Shaking in the epicentral region continued for approximately 15 to 20 seconds with ground accelerations greater than 0.05g. Peak free field accelerations reached 0.5g on rock and 1.0g on soil, exceeding those measured in the 1971 San Fernando earthquake (TMS 1994). The initial shock caused the complete collapse of many structures, including the Northridge Meadows apartments where 16 people were killed, and a parking structure at the Fashion Mall in which a man was trapped for hours under tons of concrete. Over 3500 aftershocks with magnitudes of at least 3.5, and one measuring 6.0, followed the main shock. The final human toll was 56 people killed and 7300 injured (Kosowatz 1994). Property damage estimates range between $13 and $20 billion (Ichniowski 1994) with 10,000 structures red-tagged, prohibiting entry, or yellow-tagged, signifying restricted entry (TMS 1994).

Masonry structures in the epicentral areas of Northridge and Van Nuys are mostly one-story, fully grouted reinforced concrete masonry (CMU) built within the last 20 years. Most reinforced single-story and multi-story masonry bearing wall structures sustained little or no damage. Schools, fire stations, police stations and post offices of such construction remained operational after the temblor. Older areas in nearby Hollywood, Santa Monica, Pasadena and West Los Angeles have many two- and three-story URM storefronts with parapet walls that were constructed in the early 1900's prior to the 1933 Long Beach earthquake. Most of these have been retrofitted in accordance with Division 88 and have braced parapets and through-wall diaphragm anchors.

The majority of unreinforced, unretrofitted masonry structures sustained significant damage, such as collapsed walls, fallen parapets and cracked piers. Most of these were located north of the epicenter in Ventura County, where municipalities are not subject to Division 88. For example, the town of Fillmore, approximately 20 miles northwest of the epicenter, has many 2- to 5-story unretrofitted URM residential and commercial buildings. These structures sustained some of the

worst structural damage in the earthquake. Sixty historic buildings were badly damaged, including the Masonic Temple, constructed in 1912 of hollow clay tile with brick veneer, where a section of the third-story wall and parapet collapsed. At the Hotel Fillmore, a two-story URM structure retrofitted in the first story only, parapets collapsed on the west, south and east sides. In the same town of Fillmore, a third parapet collapse occurred at the Mirage Store, an unretrofitted single-story URM structure.

Approximately 10% of the retrofitted URM structures in the epicentral area sustained significant damage (McManamy 1994). At brace points, failure of the masonry due to punching shear caused the anchors to pull out of the masonry intact. Also, out-of-plane forces resulted in numerous wall collapses. An example of such failures occurred at an automotive repair garage in Hollywood, a retrofitted structure with parapet braces and roof diaphragm anchors. The anchors held, but the adjacent 3-wythe clay brick masonry wall failed and collapsed. Another example is a coffee shop in Hollywood, a 2-story unreinforced clay brick structure with braced parapets and diaphragm anchors. Masonry adjacent to the anchors crumbled but did not completely collapse. One common denominator of such failures is evidence of poor workmanship, including partially filled head joints in the original construction.

Even some reinforced masonry buildings did not escape damage. In these structures, failures usually occurred due to construction defects, such as poor high lift grouting procedures which led to voids in areas of congested reinforcement. Inadequate bond of reinforcing bars at these locations resulted in excessive deflections and cracking. Walls that were grouted properly according to 1991 Uniform Building Code (UBC), Section 2404f performed well in the earthquake.

2.2. Modern History of URM Construction

Masonry construction in southern California of the late 1800's and early 1900's was still primarily unreinforced, and was designed and built using technology which had not been updated for decades. In contrast, the 19th century had been a time of tremendous advancement in the fields of steel and reinforced concrete design. Extensive research into masonry construction did not occur until the 1920's, when economic difficulties in India convinced officials that alternatives to concrete and steel structural systems needed to be developed. This led to research into reinforced masonry walls, slabs, beams and columns, and to a basic understanding of the structural behavior of

masonry (Beall 1984). By the late 1940's, the European community had begun in-depth studies into masonry bearing wall designs, nearly 100 years after comparable research in concrete. By this time, manufacturing processes had developed so that clay brick units were available with compressive strengths exceeding 8,000 psi and mortar compressive strengths as high as 2,500 psi.

In the United States, the first UBC, published in 1927, provided quality control standards for masonry construction, composed primarily of clay brick at that time. The code allowed the use of lime mortar for solid walls under 16 feet in height. Hollow masonry walls or walls greater than 16 feet high were required to be built with lime cement and portland cement mortars. However, the tragedy of the 1933 Long Beach earthquake brought about major changes when numerous URM school buildings collapsed, killing many children. In response, California passed the Field Act which prohibited the use of masonry in all public buildings. The next UBC in 1937 contained many new requirements for masonry construction due to the 1933 event, introducing the concept of reinforced brick masonry, and including a provision requiring use of portland cement in all mortars. The new code required that reinforcing bars be used, and that they be surrounded by grout. This requirement still exists in present codes (TMS 1994).

Masonry construction was revived in the mid 1940's and was required to follow UBC guidelines, based on reinforced concrete design practices of the period. Masonry designs were required to consider minimum lateral seismic forces and provide for reinforcement to resist tensile forces. The code also set minimum horizontal and vertical reinforcement requirements. In 1949, Los Angeles passed the Parapet Correction Ordinance which required that URM or concrete parapets above exits be retrofitted by lateral bracing or removed to minimize hazards. The results of these changes were positive as shown by improved performance of masonry structures in the 1971 San Fernando earthquake (TMS 1994).

More extreme codes such as the 1976 Long Beach city ordinance for retrofitting did not recognize any strength in URM, requiring gunite or backup concrete frames for compliance (Green 1993).

A ten-year study by the Federal Government, the City of Los Angeles and the Structural Engineer's Association of Southern California, following the San Fernando earthquake, resulted in the adoption of Division 68 of the Los Angeles Building Code on February 13, 1981. Division 68 required that all URM buildings built, under construction, or permitted for construction prior to

October 6, 1933, be retrofitted to positively anchor masonry walls to floor and roof diaphragms with parapet braces and through-wall diaphragm anchors. The Ordinance did not apply to 1- or 2-family dwellings or detached residential apartments with fewer than 5 units.

Division 68 was revised in 1985 as Division 88 to include requirements for testing and strengthening of mortar joints to meet minimum thresholds for shear strength. Division 88 also requires continuous inspection of retrofitting work. According to Mr. Larry Brugger of the City of Los Angeles Earthquake Safety Division, interviewed by telephone on May 5, 1995, 90% of the roughly 8200 URM structures in the city of Los Angeles have been retrofitted, and the remaining 10% have been demolished or vacated. However, many URM structures outside the Los Angeles city limits have not been retrofitted, and continue to be a hazard.

2.3. Division 88 of the Los Angeles Building Code

To understand the basis upon which the analytical model for this project will be developed, it is necessary to discuss Division 88 in detail. The model will represent a turn-of-the-century URM structure which has been retrofitted according to the Ordinance.

Division 88 defines an unreinforced masonry bearing wall as a masonry wall having all of the following characteristics:

1. Provides the vertical support for a floor or roof.
2. Has a total superimposed load of over 100 pounds per linear foot.
3. Has an area of reinforcing steel less than 50 percent of that required by Section 91.2418(j) of the Los Angeles Building Code. (For this project, there will be no reinforcing steel.)

Regulated structures are divided into four rating classifications: I) Essential buildings (medical facilities with emergency and surgical treatment areas, fire and police stations and disaster coordination centers); II) High-risk buildings (greater than 100 occupants, but not an essential building); III) Medium-risk buildings (greater than 20 occupants); and IV) Low-risk buildings (less than 20 occupants).

The enforcement process begins when building owners whose structures meet the criteria for regulation are served with an Earthquake Hazard Reduction Order. At that point, the owner has to employ a licensed civil or structural engineer or architect to assess the building's earthquake deficiencies and to design structural alterations to meet minimum standards for structural seismic resistance, established to reduce the risk of life loss or injury. Within 120 days, the owner must provide a plan for the installation of wall anchors, or within 270 days, a structural analysis showing that the building already complies with Division 88 or a detailed plan to meet the minimum requirements. A fourth option would be to provide a plan for the demolition of the structure.

Division 88 requires that URM walls be anchored at roof and floor levels by through-wall tension bolts (or approved equivalent) at a maximum spacing of 6 feet. Tension bolts must be anchored with bearing plates at least 30 square inches in area. Parapet walls and exterior wall appendages not capable of resisting the code-specified forces must be removed, stabilized or braced to ensure that they remain in their original position. Deteriorated mortar joints have to be raked and cleaned to remove loose mortar and then pointed with type S or N mortar. Preparation and pointing must be performed under the continuous inspection of a registered deputy building inspector certified to inspect masonry.

As part of the retrofitting planning, the strength of existing mortar has to be ascertained. This is normally accomplished through in-place shear tests or testing of 8-inch diameter cores. In-plane shear tests are performed by "shove tests" in which a brick is removed from the outer wythe of the URM wall, as well as the head joint on the opposite side of an adjacent brick. The adjacent brick is loaded horizontally until it is displaced into the space left by the head joint. The maximum applied force when lateral movement of the brick is first observed, divided by the area of the two bed joints in contact with the brick, above and below, is taken as the resulting shear stress achieved. Per Division 88, "the minimum quality of the mortar in 80% of the shear tests shall not be less than the total of 30 psi plus the axial stress in the wall at the point of the test." Figure 2.1 below is a sketch of the shove test setup. Allowances for tensile strength of the masonry are not permitted.

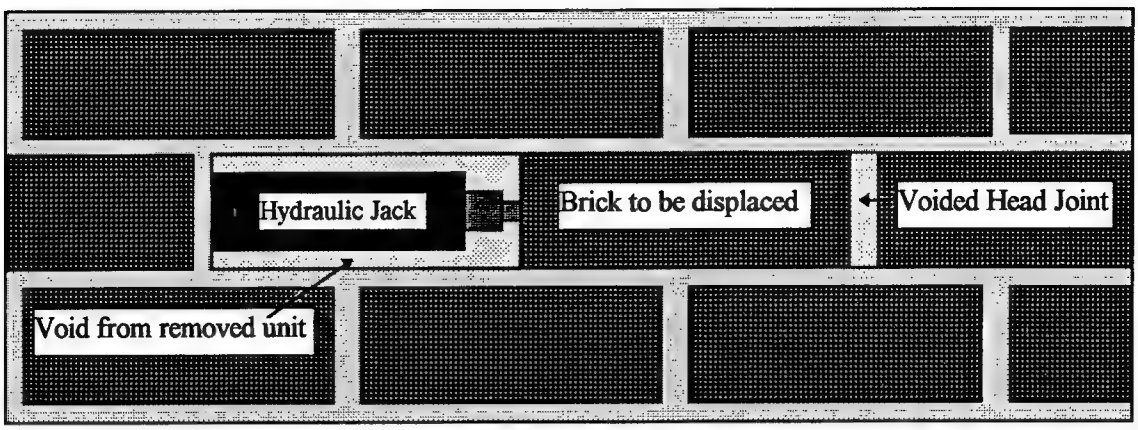

Figure 2.1: Setup for In-Plane Shear Test (Shove Test)

Time limits for completion of alterations are measured from the date the owners are served with the order. Installation of wall anchors has to be completed within one year, and complete structural alterations or building demolition has to be completed within three years of the date of the order. Time extensions of up to one year can be granted through an appeals process. Owners who fail to comply with the order are subject to having their structure ordered vacated. If the order to vacate is ignored, the owner faces prosecution by the City Attorney's office.

2.4. Other Retrofitting Techniques for URM Buildings

This project addresses only those retrofitting techniques prescribed by Division 88 of the Los Angeles Building Code. Other methods are also available, though less proven. Those are discussed briefly below.

Center-core strengthening is a technique whereby holes (normally 4-in. diameter) are cored vertically through an existing URM wall at various spacings (6 or 8 feet) from the top down into the footing. A single #6 to #9 bar is placed in the cored hole, and the cavity is grouted. The reinforcement is designed so that the representative wall sections will be under-reinforced (i.e., yielding of steel will occur before crushing of masonry). The result is a nearly homogeneous structural element fully tied to the foundation, with increased shear and bending capacity. Advantages of this technique are that it does not alter the appearance of the wall (which makes it

preferable for retrofitting of historic buildings), and that the work can be accomplished while the user remains in the building. The process was developed in 1984 with the assistance of a grant from the National Science Foundation (Breiholtz 1993).

Full-scale testing of the center-core technique was performed in Long Beach, California on a one-story URM building scheduled for demolition for the 1984 Los Angeles Summer Olympic Games. Tests of in-plane shear and out-of-plane bending strength were conducted using various core diameters, reinforcing bar sizes and grouts. Results showed that the sections with polyester and epoxy grouts performed better than those with other grouts. Grout migration into the inner and outer wythes was evident upon inspection during building demolition. Grout migration and strong masonry/grout bond resulted in high in-plane shear strength and out-of-plane bending strength.

The results of the study cleared the way in Long Beach for more widespread use of the technique. One such project was a large-scale retrofit with approximately 4400 linear feet of coring for a church in Long Beach, built around 1913. However, no actual earthquake performance data were presented in the reference for the structure after retrofitting.

Another retrofitting method is the addition of reinforced concrete to one or both sides of a URM wall to increase in-plane shear resistance and out-of-plane bending strength through membrane action. This method alters the appearance of the wall, and would not be suitable for retrofit of historic buildings where the original architectural appearance must be maintained. Also, such retrofitting work is extremely disruptive to building occupants.

A large retrofit project at the University of California, Berkeley combined the techniques described above along with diaphragm upgrades to strengthen South Hall, constructed in 1873 (Campi 1989). Shotcrete was placed on walls at each end of the building to create shear walls capable of resisting the total anticipated lateral seismic force on the structure. Five-inch diameter center-cores were bored in the brick walls and filled with reinforcement and polyester resin grout to provide out-of-plane strength. Walls were anchored to diaphragms with adhesive dowels, since through-wall anchors would have been aesthetically unacceptable for this historic building. Extensive diaphragm upgrades included replacing the wood flooring with steel decking topped with reinforced concrete, supported by a new steel truss along the central corridor. URM chimneys were

completely filled with concrete above roof level. Again, no data was presented on the post-retrofit earthquake performance of the structure.

Post-tensioning of existing URM walls was attempted in 1969 at Audubon High School in Los Angeles (Breiholz 1993). The process was unsuccessful because the wall could not maintain the tension in the strands due to excessive deformations. Thus, no precompression of the masonry remained. This technique has not been shown to be a viable option for seismic retrofitting.

CHAPTER 3: DEVELOPMENT OF ANALYTICAL MODEL

3.1. Prototype URM Structure

The prototype URM structure examined in this project was a 3-story URM bearing wall building with a square plan of 40 ft by 40 ft. The walls are 3-wythe clay brick with a thickness of 12 inches, including a veneer wythe. Floor and roof diaphragms were assumed to be timber, as in many turn-of-the-century masonry structures. Figure 3.1 below is an illustration of the prototype:

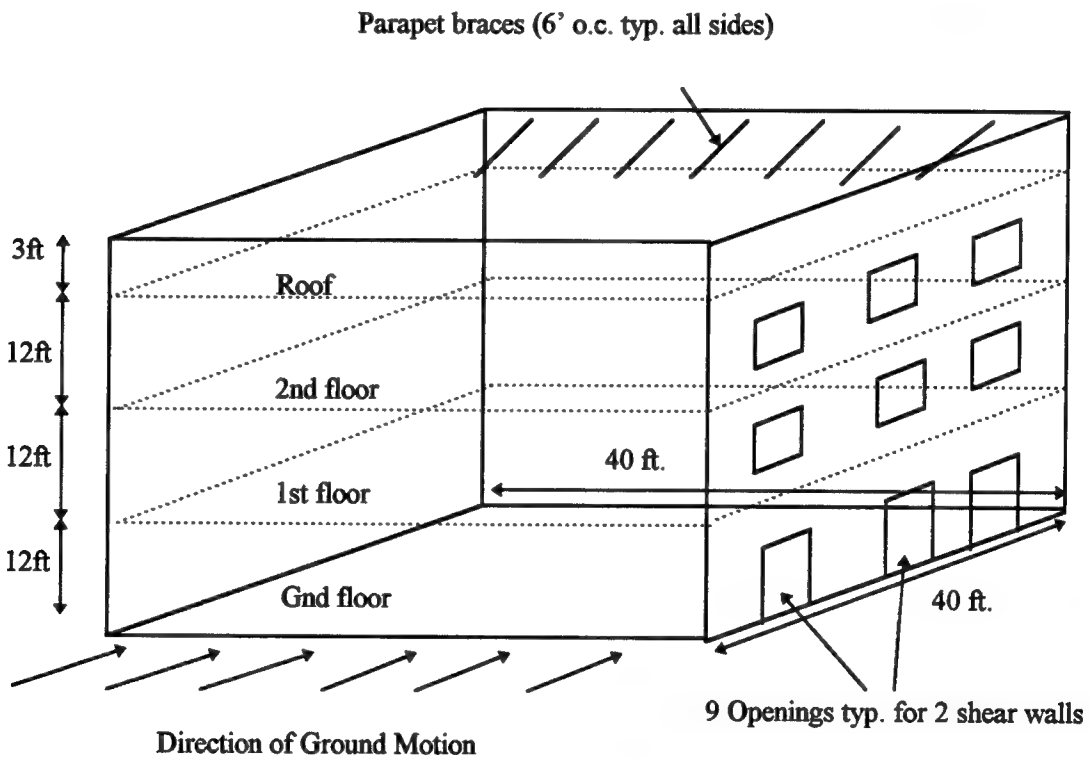

Figure 3.1: Prototype URM Structure

To calculate the response of the prototype to a representative earthquake, an analytical model was developed using techniques and assumptions employed by similar research in the past. For example, Abrams and Tena-Colunga (1993) studied a 2-story 1890's vintage URM firehouse located 15 km from the epicenter of the 1989 Loma Prieta, California earthquake. The structure is a 3-wythe clay brick bearing wall building with timber diaphragms, approximately 40 by 60 ft. in

plan. That team utilized a sophisticated 3-dimensional finite element model and the ABAQUS program using thick shell, isoparametric 8-noded elements. They assumed linear behavior, since the structure was virtually uncracked following the earthquake. Dynamic loading was provided in the form of a time history from measured ground motions and analyzed by time step integration of 20 modal coordinates.

Kingsley, Kurkchubasche and Seible (1993) used a non-linear, three-dimensional finite element model in analyzing the response of a 5-story concrete masonry structure, employing 4- and 8-noded isoparametric plane stress elements for shear walls.

Studies by Jalil, Kelm and Klingner (1992) were conducted on several different types of buildings involved in the 1989 Loma Prieta earthquake. Their analysis of the Loma Prieta Community Center was performed using the SAP90 Structural Analysis Program. The element chosen for the analysis of the reinforced masonry bearing walls in the structure was the 3-dimensional shell element that reproduces out-of-plane bending and in-plane membrane action. Plywood roof diaphragms and shear walls were modeled with membrane elements having in-plane stiffness only. For the Hotel Woodrow, a steel frame structure with masonry infill and veneer located in Oakland, California, masonry walls were analyzed with combinations of vertical and spandrel wall finite elements.

Tomazevic (1987) conducted a study that considered both the linear behavior of masonry before cracking and the non-linear behavior after cracking. He used two analytical models, including a four-degree-of-freedom shear system and an equivalent single-degree-of-freedom system. Both utilized hysteresis records to model degradation in stiffness. His prototype was a four-story partially reinforced masonry structure with rigid diaphragms. A scale version of the prototype was tested in the laboratory on a shaking table.

3.2. Material Properties

Material properties for the current project were derived from those used in similar studies. For example, Jalil et al. estimated a timber diaphragm weight of 21 psf and a live load of 28 psf in their analysis of the Hotel Woodrow, assuming that 70% of the Code prescribed live load would be

present during an earthquake. They used a modulus of elasticity of 1500 ksi and a shear modulus of 625 ksi for timber. For masonry, they assumed a density of 120 pcf, a modulus of elasticity of 1600 ksi and a shear modulus of 640 ksi.

Kariotis and Nghiem (1993) conducted tests on masonry infill panels in Los Angeles. Although the current research project is not concerned with infill panels, the type of walls they tested were of the same construction as those of the prototype for this project (i.e., 3-wythe, header-bonded clay brick with partially filled head and collar joints). The team performed flat-jack compression tests in-situ on two buildings at 219 S. San Pedro St. and Second & Central Streets. Ages of the buildings were not provided in the reference. Flat jacks were inserted into bed joints which had been saw cut to create a void. Prisms tested were 5 courses high and were compressed at various angles. The tests showed mean secant modulus values of 0.77×10^5 psi at Second & Central and 1.10×10^5 psi at 219 S. San Pedro St. A comparable study by Guh and Youssef (1993) used flat-jack and prism tests in the field to determine in-place compressive strengths. Their study found lower compressive strengths than did Kariotis and Nghiem as reflected in a mean secant modulus value of 0.45×10^5 psi.

Further documentation of such tests was found in a report by Cousins, O'Connor and Plecnik (1986), regarding center-core strengthening tests conducted at California State University, Long Beach and North Carolina State University. In-place compression and shear tests were performed on a building built in 1890 with lime cement mortar and another building constructed in 1915 with what the reference called a "type N cement mortar". Both structures showed signs of poor workmanship, including partially filled collar joints. In-plane shove tests gave average shear strengths of 28 psi in the 1890 building and 49 psi in the 1915 building. Compressive strengths, compiled only for the 1915 structure, averaged 534 psi, and were used to estimate an average modulus of elasticity of 534,000 psi.

Finally, tests by Mengi and McNiven at the University of California at Berkeley (1989) considered linear behavior before cracking, as well as the non-linear behavior of URM after cracking, in the formulation of an analytical model for predicting the response of a URM structure. They used a shear modulus of 24.4 ksi before cracking, and 0.13 ksi after cracking.

Based on the above data, material properties were selected for the current project that were most representative of those materials used prior to 1933 in southern California, considering the affects of poor workmanship, age and prior earthquakes. To be conservative, worst-case values were selected, including a modulus of elasticity (E) of 450 ksi, and a shear modulus G = 24.4 ksi. A Poisson's ratio of 0.35 was used for masonry to account for the impact of shear deformations. Masonry density was assumed as 120 pcf. A timber diaphragm weight of 22 psf with applied live loading of 28 psf was assumed. Quantities of weight were divided by the acceleration due to gravity of 32.17 ft/sec^2 to obtain mass units.

3.3. Development of Computer Model

The prototype structure was modeled and analyzed with 2 different models, using the SAP90 Structural Analysis Programs. SAP90 was selected for its versatility and convenience in creating 2- and 3-dimensional finite element models. The software conducts dynamic earthquake response analysis using time history or response spectra input. The user can choose either an eigenvalue or a Ritz Vector analysis to obtain the number of mode shapes requested in the input data. The program solves the eigenvalue problem using an iterative solution method called an "accelerated subspace iteration" algorithm which starts with approximate eigenvectors and iterates until the eigenvectors converge. In the time history mode, the mode shapes are then integrated using Constant Average Acceleration method and combined by modal superposition (Habibullah 1990).

The first SAP90 model was a simple 2-dimensional vertical cantilever beam, programmed to provide a baseline set of results for comparison with the larger model to follow. Three vertical beam models were prepared, consisting of varying numbers of frame elements connecting nodes at and between the floor levels. Gross section properties for moment of inertia, shear area, etc. were input for each floor level. One half of the wall area of those walls subjected to out-of-plane bending was removed for calculation of the moment of inertia due to the fact that it would contribute little to the lateral stiffness of the structure. Figure 3.2 below is a sketch of the three vertical beam models analyzed.

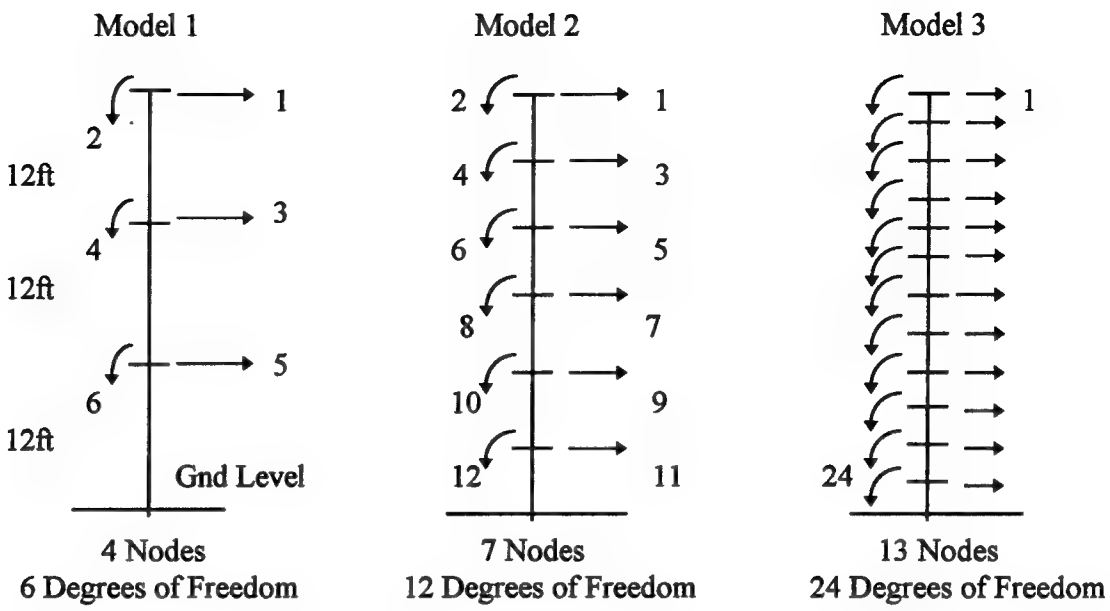

Figure 3.2: Vertical Cantilever Beam Models using Frame Elements

The 3 models were initially run using the N-S component of the 1940 El Centro earthquake at both 2% and 5% damping. This was done to test the sensitivity of the models to damping changes and to the addition of more elements per story. The variation in results from the different damping values was negligible. Thus, only 2% damping was applied to subsequent analyses. As more elements were added, however, the model became less stiff, experiencing larger tip deflections and accelerations. The 13-node model was selected for analysis with the Northridge data because it provided the highest tip displacement and acceleration results of the 3 models tested. Appendix A contains the SAP90 data file for the 13-node vertical beam model.

For the larger 3-dimensional model, a complete finite element reproduction of the structure was created. Since the parapet is braced, the extension above roof level was neglected and only its mass was considered. Also, due to the large number of elements required to model the entire structure, the building was cut in half to stay within the constraints of the educational version of the software. The nodes along the cut edge were restrained from translating horizontally normal to the direction of ground motion, but were free to translate horizontally parallel with the ground motion and vertically. Rotations were fixed other than in the overturning direction of the ground motion. Representative openings were provided in the form of 3 doors at ground level and 3

windows at the first and second floors. Figure 3.3 below shows the undeformed geometry of the model, consisting of 63 nodes and 66 elements. Appendix B contains the SAP90 data file for the 3-dimensional model and a SAPLOT drawing of the finite element mesh in Figure B-2.

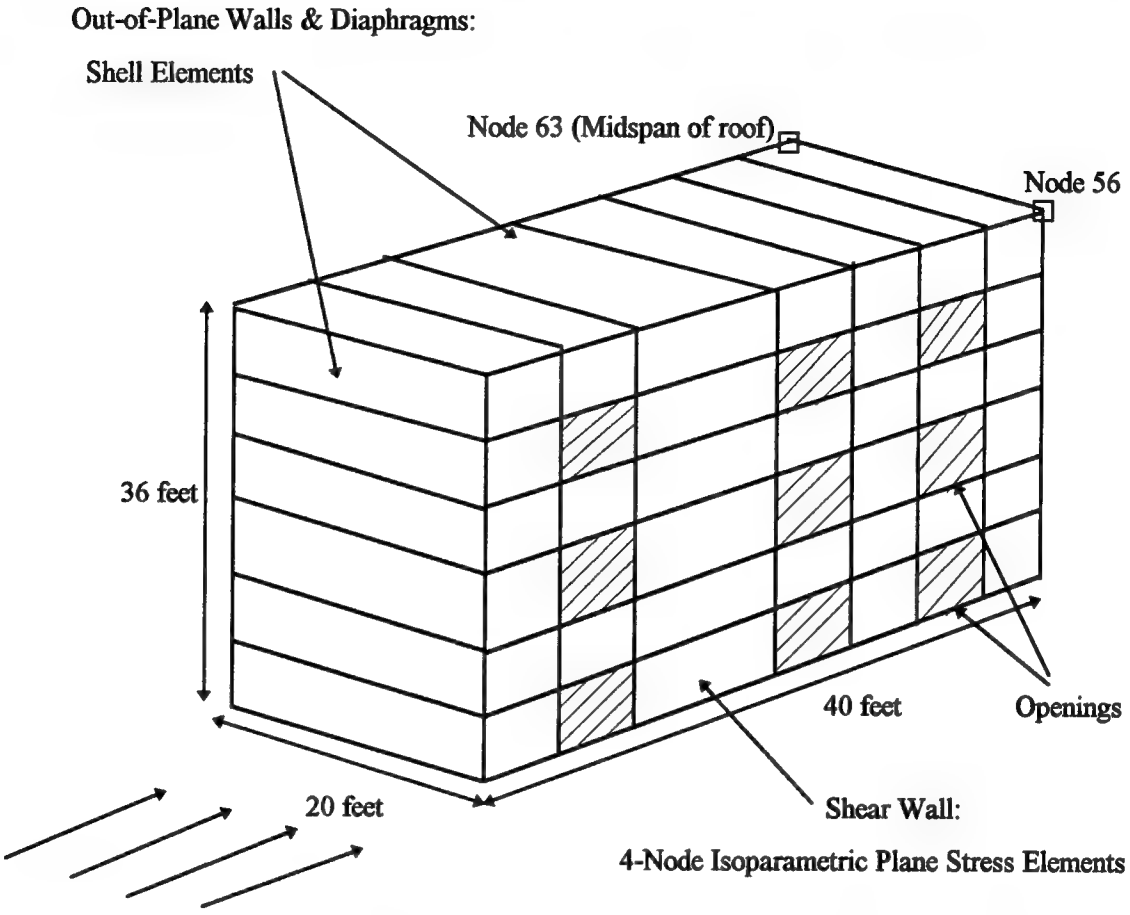

Figure 3.3: Undeformed Geometry of 3-Dimensional SAP90 Model

The SAP90 4-noded isoparametric shell element was used for diaphragms and walls subjected to out-of-plane bending. The element formulation includes a combination of plate bending and membrane behavior, making it a very versatile element. The membrane formulation includes translational in-plane stiffness components and a rotational stiffness component normal to the plane of the element. Plate bending behavior includes two-directional out-of-plane plate rotational stiffness components and a translational stiffness component in the direction normal to the plane of

the element. Stresses in all of the selected elements are calculated at the Gaussian integration points and extrapolated to the nodes (Habibullah 1990).

Although the SAP90 shell element is versatile, it is designed primarily for modeling structures whose behavior is controlled by out-of-plane bending. It tends to be artificially stiff with respect to in-plane deformations (Habibullah 1990). The response of the prototype structure for this project was controlled by the in-plane behavior of the shear walls. Thus, the shell element was inappropriate for this purpose, resulting in unreasonably small displacements at the roof level of the model (approximately 0.1 in.). To more accurately reflect the contribution of the shear walls, they were modeled using SAP90's 4-noded isoparametric, plane-stress membrane element. The incorporation of this element increased maximum computed roof deflections to 1.25 in., more reasonable for the prototype structure.

3.4. Input Loading

The east-west component of the 1994 Northridge, California earthquake served as the dynamic loading for the models. The data were recorded from ground motions measured at the Santa Monica City Hall during the event. The analysis was run with a time history of the earthquake, assuming 2% damping. Figure 3.4 below is a plot of the input record.

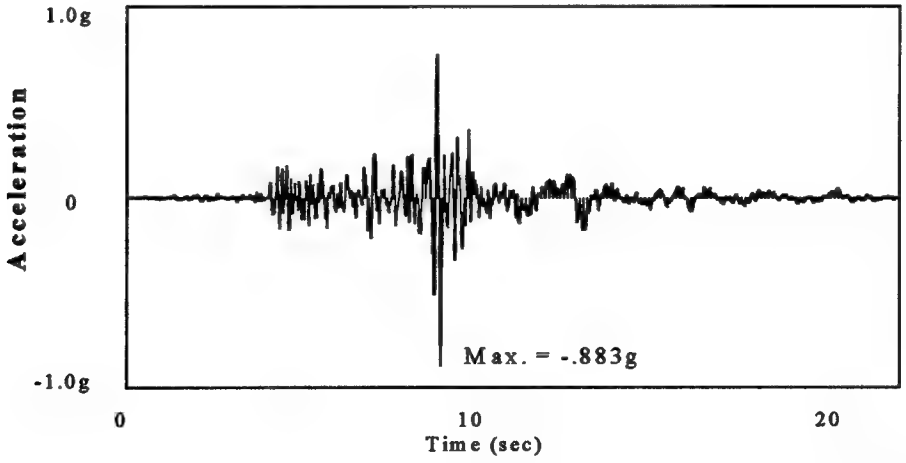

Figure 3.4: Input Record; E-W 1994 Northridge, California recorded at Santa Monica City Hall

CHAPTER 4: RESULTS OF ANALYSIS

4.1. Overview of Results

The first model analyzed was the 13-node, 2-dimensional vertical cantilever beam, using the Northridge 1994 time history input. Results of the eigenvalue analysis of the first 20 mode shapes are included in Appendix A. The first mode contributed most to the maximum response of the model. Participating mass in the first mode consisted of 85.6% of the total mass of the structure in the horizontal (X) direction. By the thirteenth mode in the eigenvalue analysis, 100% of the mass was participating in the X direction. Therefore, the modes analyzed adequately represent the response of the model.

Figure 4.1 below is a tip displacement time history plot generated by the SAPTIME program.

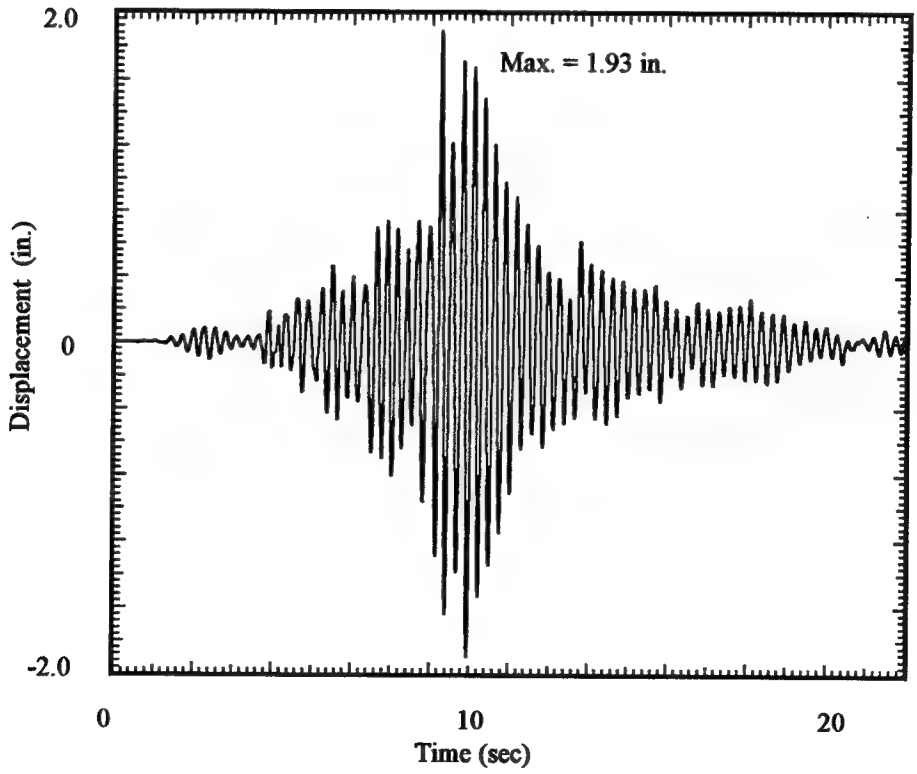

Figure 4.1: Tip Displacement Time History for Vertical Beam Model

The fundamental period of the structure was calculated as 0.32 sec. with a maximum tip displacement of 1.93 in. The model experienced a peak tip acceleration of 2.18g (70.1 ft/sec^2). The peak displacement and acceleration responses followed a sharp spike in the ground accelerations during the earthquake, occurring at approximately 9.8 seconds into the record (refer to Figure 3.4). Until that point, peak ground accelerations had reached slightly more than 0.2g, then abruptly peaked to nearly 0.9g, causing a dramatic response in the computer models. Figure 4.2 below is a time-history plot for tip acceleration of the 2-dimensional model.

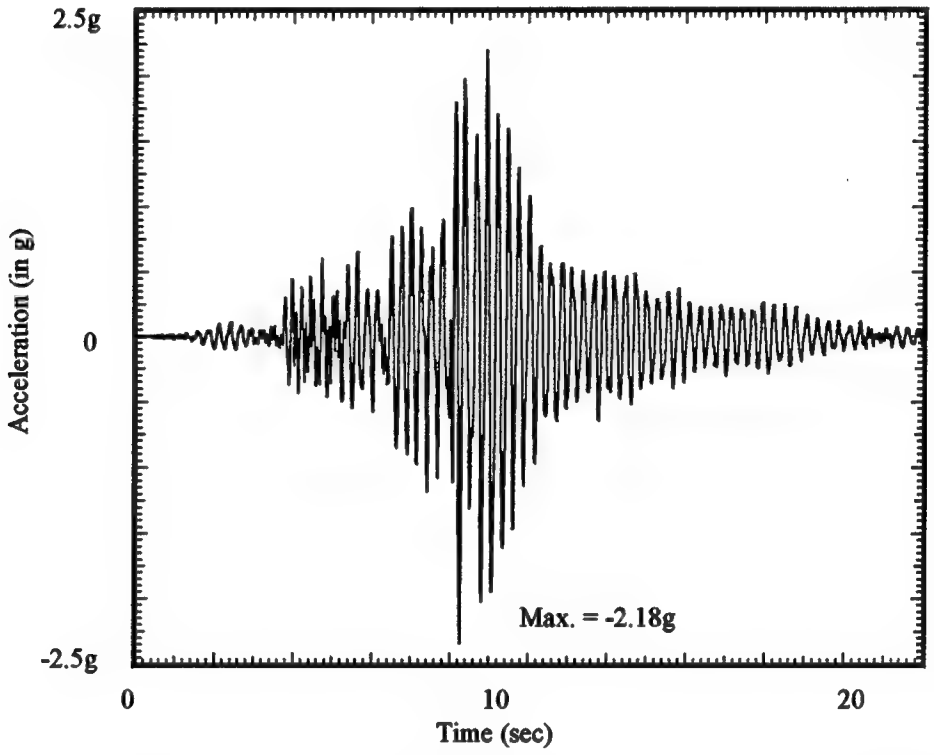

Figure 4.2: Tip Acceleration Time History for Vertical Beam Model

As shown in the acceleration plot, the vertical beam tip acceleration response is very small (approximately 0.1g) until around 4 seconds into the record, when ground accelerations suddenly increased to 0.2g. This increase caused a roughly linear increase in tip acceleration to 0.8g. Then, at the time of the spike in ground acceleration, tip acceleration suddenly increased nearly 3-fold from 0.8g to the peak of 2.18g. The response then smoothly decreased to approximately 0.1g by the end of the input record.

Next, the 3-dimensional finite element model was run with the Santa Monica input record. Appendix B contains selected information from the SAP90 analysis of the model, including results of the eigenvalue analysis of the first 20 mode shapes. Figure B-1 is a plot of the fourth-mode deformed shape, primarily responsible for the maximum lateral response of the model. In this mode, 85.2% of the total mass of the structure was participating in the X direction, the direction of ground motion. For the 20 modes analyzed, 98.5% of the total mass was participating in the X direction. This is a lower percentage than with the 2-dimensional vertical beam model, primarily because of the vertical oscillations of the diaphragm masses in the 3-dimensional model. This did not occur in the 2-dimensional model since diaphragm masses were lumped at nodes, able only to translate in the X direction. This is also the reason for the greater response of the 2-dimensional model, as will be discussed in Chapter 6.

Figure 4.3 below is a time-history plot of the displacement response at Node 63, the midspan of the roof along the edge away from the direction of ground motion (refer to Figure 3.3).

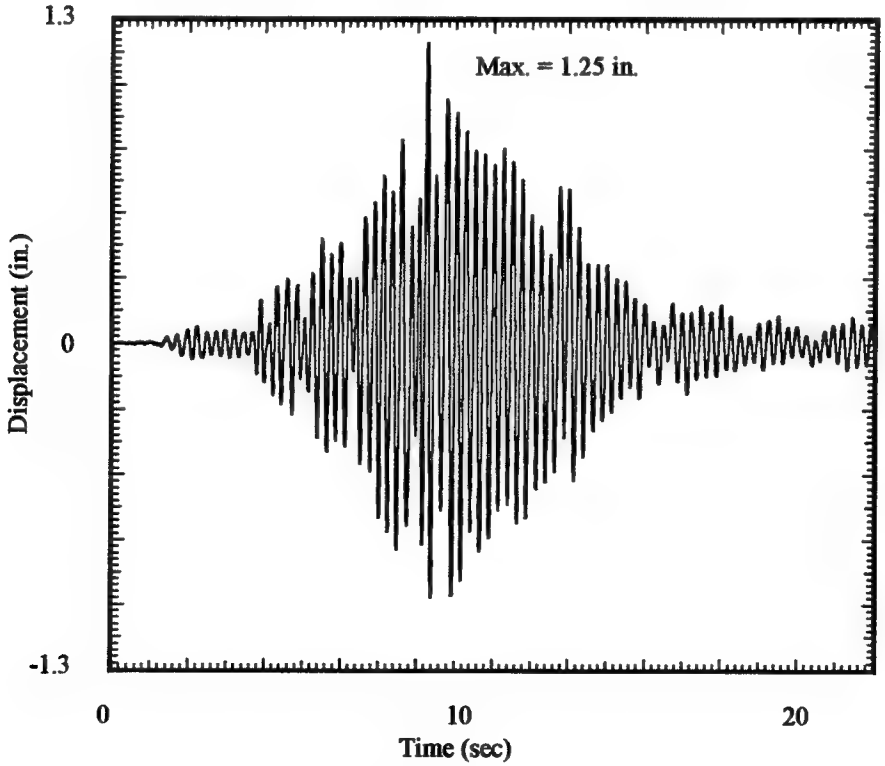

Figure 4.3: Displacement Time History for 3-D Model (Node 63)

The response of the 3-dimensional model was quite different from that of the vertical beam model. The 3-dimensional model had a fundamental period of 0.29 sec., slightly smaller than that of the simplified vertical beam model. Maximum tip deflection was 1.23 in. and the peak tip acceleration was 1.64g, significantly lower than the corresponding responses of the vertical beam. The models will be compared in more detail in Chapter 6.

Figure 4.4 is a tip acceleration time history plot for node 63 of the 3-dimensional model. Similar to the vertical beam response, tip acceleration at the midspan of the roof increased steadily from about 0.1g at time (t) = 4 seconds into the record, to just over 1.0g before the spike in ground acceleration. When the spike occurred, the response peaked to 1.64g, and then smoothly decreased to approximately 0.2g for the remainder of the input record.

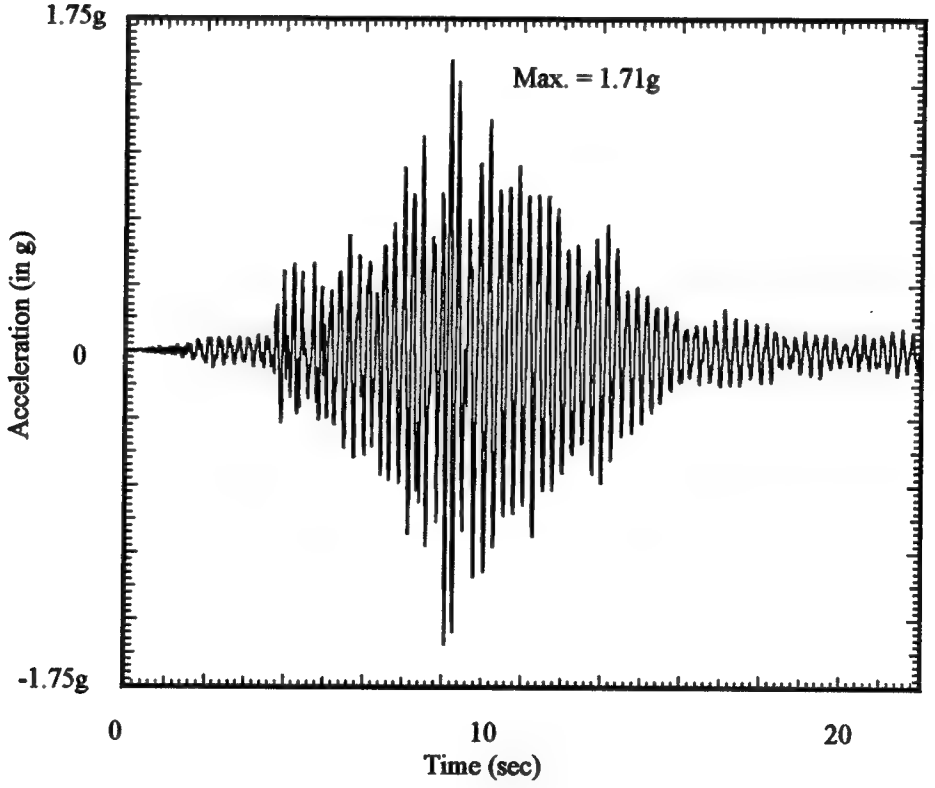

Figure 4.4: Acceleration Time History for 3-D Model (Node 63)

4.2. Verification of Results

To assess the reasonableness of the results obtained in the SAP90 analyses, a response spectrum of the input record was generated using the SPECTRA program. A plot of the spectrum is shown below in Figure 4.5.

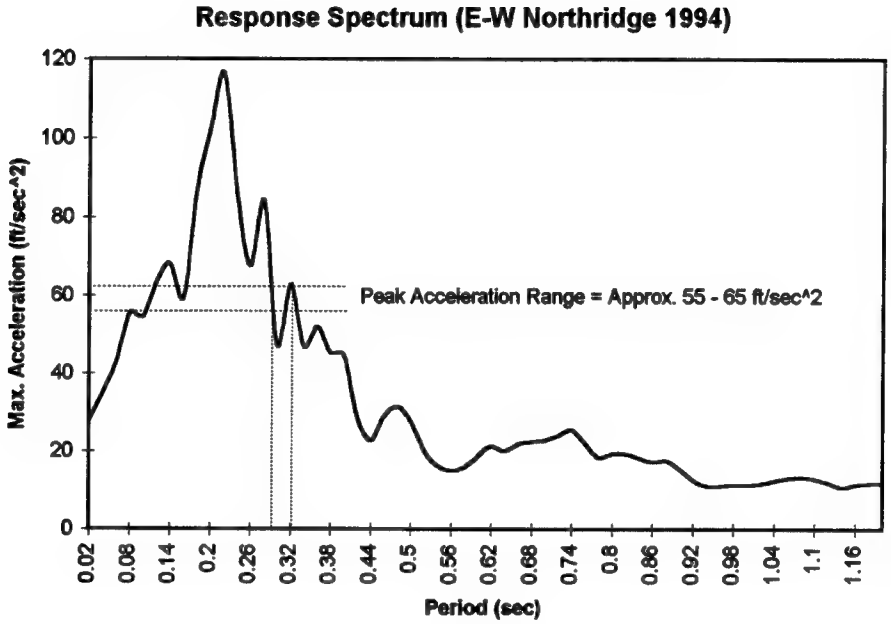

Figure 4.5: Response Spectrum for E-W Northridge Input Record

The range of maximum acceleration values for fundamental periods of 0.29 to 0.32 seconds is approximately 55 to 65 ft/sec^2 respectively. The values obtained from the SAP90 analyses were 52.8 ft/sec^2 and 70.1 ft/sec^2 for the periods of 0.32 sec and 0.29 sec respectively. Considering the accuracy of the spectrum plot and the inexact nature of plotting the fundamental periods in Figure 4.5, the values of maximum acceleration obtained from SAP90 fall within the expected range of values per the response spectrum. Thus, the results are reasonable.

CHAPTER 5: APPLICATION OF RESULTS

5.1. General

In this chapter, results from both the 2-dimensional vertical beam and the 3-dimensional finite element models are used to calculate a dynamic loading history and to design the loading apparatus for the experimental phase of the project. Figure 5.1 below is a sketch of the laboratory specimen setup for the experimental phase. This setup will simulate a parapet at the roof level of a 3-story URM building subjected to earthquake excitation. Four such specimens will be prepared. One baseline specimen will be built and braced according to the current Division 88 requirements, but with no further improvements. The other three will contain one or more retrofitting modifications, including grout injection of masonry cracks and/or metal ties, drilled and grouted into the existing masonry to bind existing wythes together.

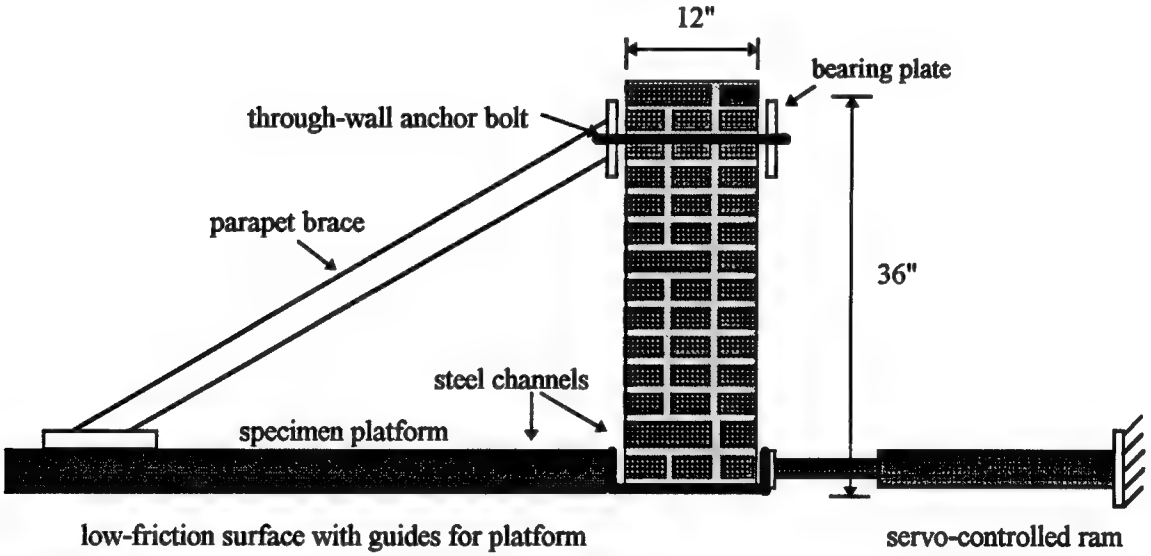

Figure 5.1: Laboratory Specimen: 3-Wythe Header-Bonded Wall with Veneer

After dynamic loading, the condition of the wall specimens will be assessed to determine which retrofitting technique most improved the earthquake performance of the wall. These techniques will be recommended for inclusion in future revisions to the City of Los Angeles Building Code, Division 88. A more detailed report from the experimental phase of the project will be published at a later date in the form of a Master's Thesis.

5.2. Calculation of Dynamic Loading

To apply the calculated results presented in Chapter 4 to a practical laboratory experiment, a more useful form of the information was required. The acceleration response time histories had to be converted to a single idealized sinusoidal response history, easily programmable for a servo-controlled ram. Also, time histories of velocity and displacement were necessary for calculation of ram requirements (i.e. oil pumping rate and stroke requirements).

To obtain an idealized acceleration history, representative data peaks were obtained from the 3-dimensional model acceleration response time history. This response more closely resembled a sinusoid than did the 2-dimensional model response. Then, separating ascending and descending data for regression analysis, the data were plotted using Microsoft EXCEL, and best-fit exponential trendlines were applied. The exponential functions were then normalized to have a maximum acceleration response of 2g at a time of 10 seconds. This idealized peak amplitude is an approximate average of the maximum acceleration responses of the 2- and 3-dimensional models. The best-fit curves, calculated and normalized to a maximum acceleration of 2g, are shown in Figure 5.2 on page 28.

Using the idealized exponential functions, and assuming a response period of 0.3 seconds from an average of the 2 computer models, a sinusoidal acceleration loading history was calculated with the following relationship:

$$\ddot{U}g(t) = 2g \text{ Sin } pt \text{ , where: } p = \frac{2\pi}{0.3}$$

To obtain a velocity time history to be used for calculating hydraulic oil pumping rates for the ram, the above expression was integrated once, resulting in the following equation:

$$\dot{U}g(t) = \left(\frac{2g}{p}\right) \text{ Sin } pt$$

Finally, to calculate ram stroke requirements, the equation was integrated once more to obtain the following function for displacement:

$$Ug(t) = \left(\frac{2g}{p^2}\right) \text{ Sin } pt$$

The resulting idealized acceleration, velocity and displacement plots are shown in Figure 5.3 on page 29.

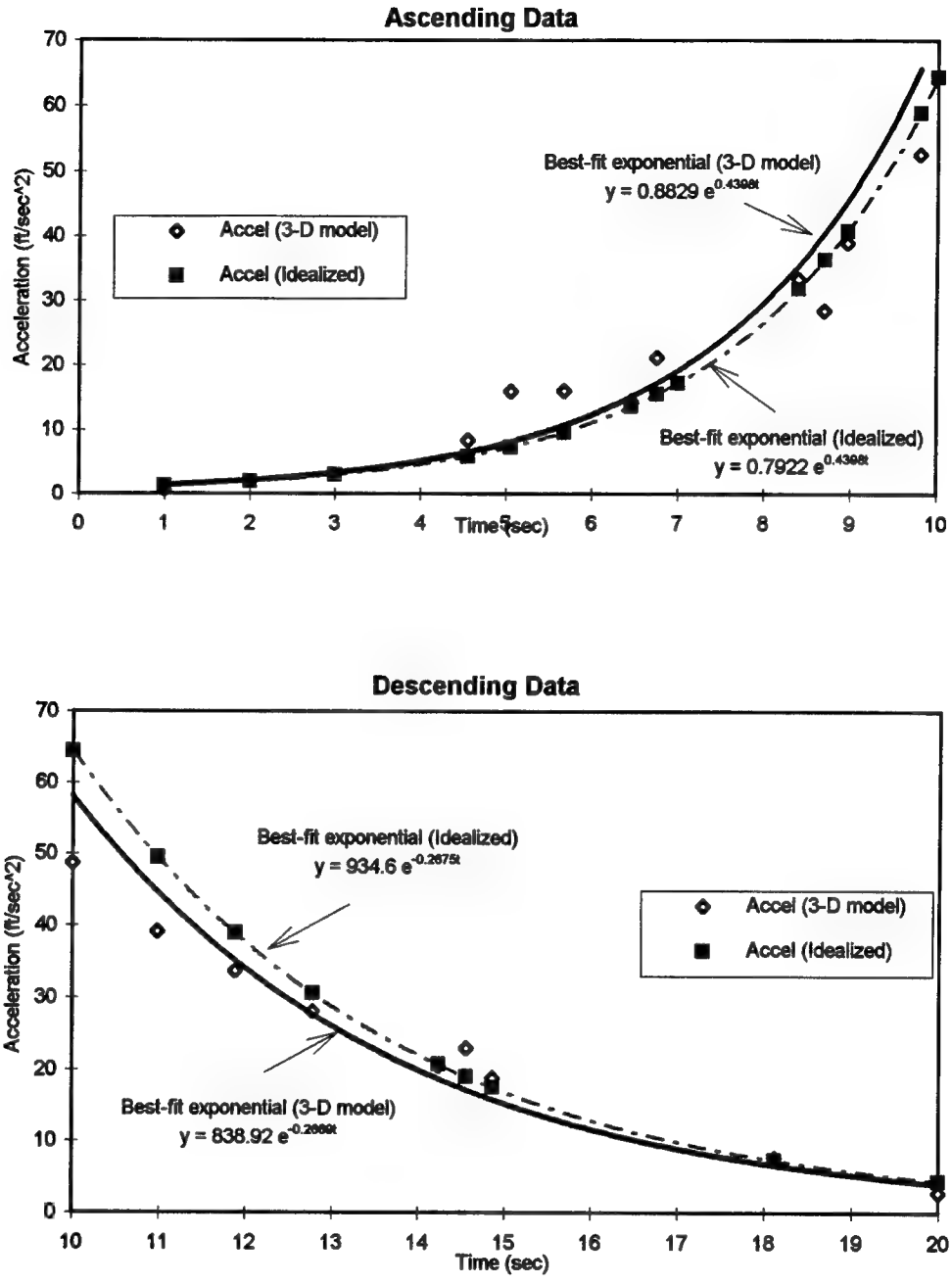

Figure 5.2: Idealized Envelope Curves for Ascending and Descending Acceleration Data

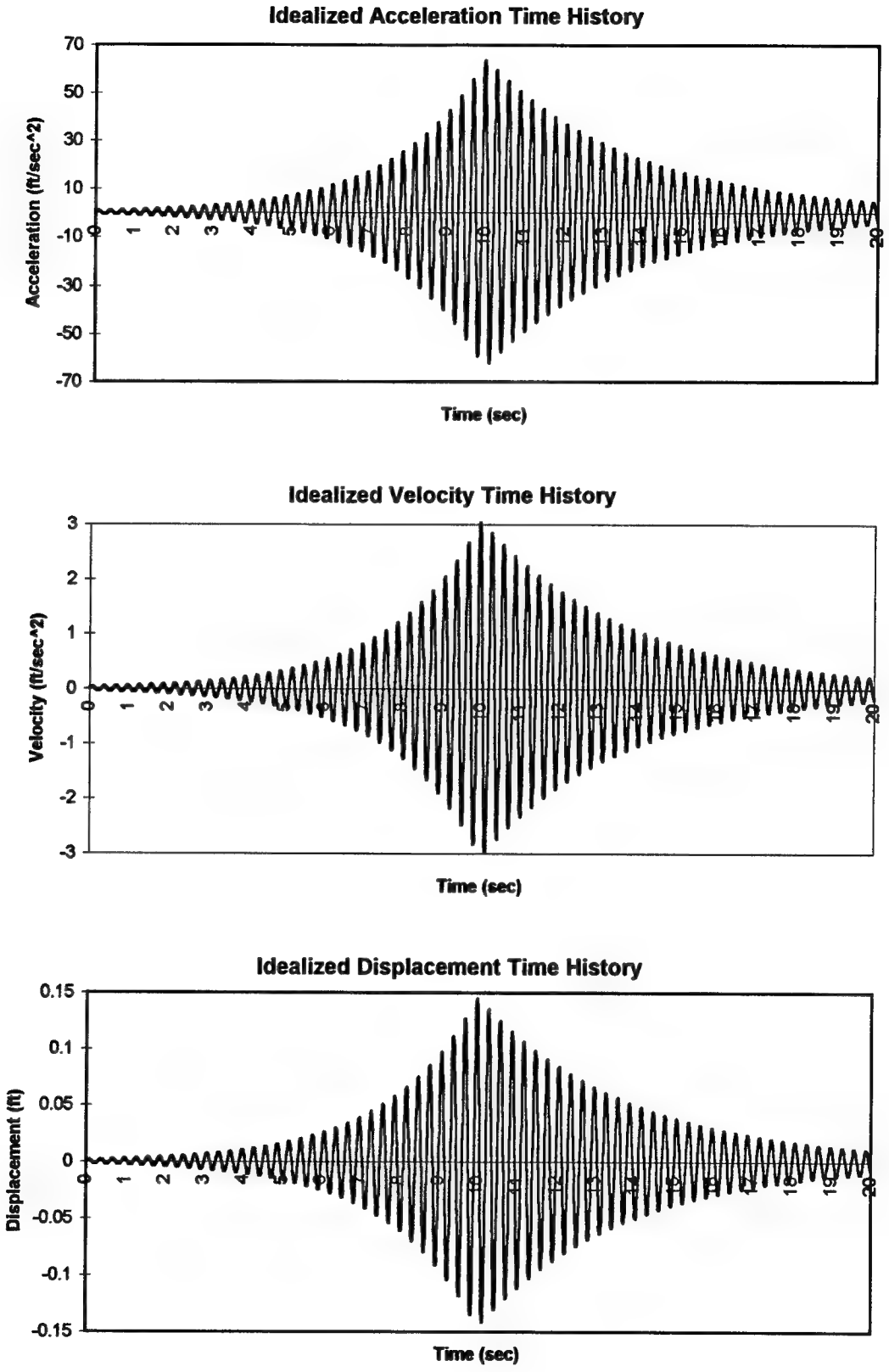

Figure 5.3: Idealized Loading Curves for Laboratory Specimens

CHAPTER 6: SUMMARY, CONCLUSIONS AND RECOMMENDATIONS

6.1. Summary

Improved performance from seismic retrofitting of unreinforced masonry (URM) buildings has been well documented. A study conducted after the 1987 Whittier Narrows, California earthquake found that complete retrofitting of URM buildings in accordance with established criteria significantly reduces earthquake damage at moderate ground motions (Bruce 1993). That study examined a database of 113 structures, 81 of which had been completely retrofitted in accordance with the Los Angeles Building Code (Division 88), the San Francisco Building Code (section 104f) or other applicable codes. The other 32 had been partially or arbitrarily retrofitted with no known criteria. The study also concluded that arbitrary or incomplete retrofitting did not significantly improve performance under moderate ground motions nor improve life safety under large ground motions.

The purpose of this report was to introduce a project that intended to improve current retrofitting techniques prescribed in the City of Los Angeles Building Code, Division 88. As per the objectives set forth in Chapter 1, the Northridge earthquake was discussed to provide a background on the event which led to the inception of this project. Current retrofitting technologies and those prescribed by Division 88 were also reviewed.

In Chapter 3, the theoretical background of the structural dynamic problem and modeling of the prototype structure were discussed. Two models were introduced, including a 2-dimensional vertical beam model and a 3-dimensional finite element reproduction of the prototype structure. The models were created and analyzed with the SAP90 Structural Analysis Programs, a very fast and convenient software package for conducting finite element analyses. The software automatically calculates the stiffness for each finite element independently, then assembles a structure stiffness matrix from the individual elements. Shear deformations and localized deformations are automatically calculated within the program.

The two models were formed very differently. For example, the simplified model was a 2-dimensional vertical cantilever beam, consisting of frame finite elements with limited degrees of freedom for horizontal translation and rotation in the overturning direction only. Wall masses were distributed along the length of the frame elements, and diaphragm masses were lumped at the nodes corresponding to floor levels. Moments of inertia for the frame elements were calculated using the gross plan of the structure with one half of the cross wall area removed due to fact that it would contribute little to the lateral stiffness of the building. Shear area used was the total area of the two shear walls minus the area of the window and door openings. Modulus of elasticity and shear modulus values were the same for both models.

The 3-dimensional model was constructed using shell and plane stress finite elements. Material properties, including unit mass, modulus of elasticity and shear modulus values were entered for each material type used in the model. The input data specified the location, size and type of the finite elements in the mesh. All other properties, including moment of inertia, were calculated automatically by the program for each element, and were assembled for the entire structure. Variations in geometry of the structure were much more accurately represented in the 3-dimensional model.

The results of the SAP90 analyses of the 2 models and application of those results were discussed in Chapters 4 and 5. Excerpts of the computer output are provided in the appendices.

6.2. Conclusions

The 3-dimensional finite element SAP90 model provided a more accurate representation of the prototype building than the 2-dimensional vertical cantilever beam model because it more exactly reproduced the geometry and degrees of freedom of the actual structure. The vertical beam model was an idealized structure with few degrees of freedom and gross section properties. It provided similar results to the larger model. However, maximum displacement and acceleration responses of the 2-dimensional model were significantly higher than the 3-dimensional model.

The 3-dimensional model analysis resulted in a maximum roof displacement of 1.23 in. and a maximum acceleration of 1.64g ($52.8 ft/sec^2$) at midspan of the roof. In contrast, the vertical

beam model experienced a maximum tip displacement of 1.93 in. and a maximum tip acceleration of 2.18g (70.1 ft/sec^2). This is an increase of 57 percent for tip displacement and 33 percent for tip acceleration over the 3-dimensional model.

The fundamental period of the vertical beam model (0.32 sec.) was slightly longer than that of the 3-dimensional model (0.29 sec.). This was due to the fact that the diaphragm masses in the 2-dimensional model were lumped at the floor levels. These masses could only translate horizontally with the direction of ground motion. As a result, most of the mass of the structure participated in the first response mode, increasing the period of the structure. In contrast, the response of the 3-dimensional model was greatly affected by vertical oscillations of the diaphragms. In fact, these oscillations dominated the first 3 modes of response. The simplified geometry and section properties of the vertical cantilever beam model minimized the effect of the distributed mass of the diaphragms.

Although the results from the 2 models differ as described above, the maximum accelerations obtained in the analyses are both reasonable as verified in Chapter 4 by a check of the response spectrum of the input record. The idealized acceleration, velocity and displacement time histories calculated in Chapter 5 provide a programmable approximation of the response of the prototype building to the given input record. This data will be programmed as the dynamic loading for the laboratory specimens, simulating the loading on an actual parapet of the prototype building.

3.3. Recommendations

The analysis presented in this report was limited in scope due to the fact that extreme accuracy was not required, and also by software constraints of the educational version of the SAP90 software. Future researchers may wish to perform such an analysis with a complete modeling of the structure, including more accurate diaphragm modeling with floor beams and sheathing represented by separate finite elements. Diaphragm action had a tremendous impact on the overall response of the structure. Also, soil/structure interaction was not considered in the models of this report. Ground motions recorded at the Santa Monica City Hall were assumed to be directly imparted to the foundation of the prototype URM structure in this project.

Investigation of the affects of grout injection in the laboratory phase of this research project will provide useful information for improving the retrofitting provisions of Division 88 of the City of Los Angeles Building Code. However, further research will be required before a complete understanding is achieved of the seismic behavior of URM structures and of the best retrofitting actions for such structures.

REFERENCES

Abrams, D.P. and Tena-Colunga, A., 1993. "New Views for Modeling Dynamic Response of URM Buildings," Structural Engineering in Natural Hazards Mitigation, Proceedings of Papers Presented at the Structures Congress '93, ASCE, Irvine, California, 1993, pp. 1191-1196.

Beall, C., 1984. Masonry Design and Detailing for Architects, Engineers and Builders, Prentice Hall, Inc., Englewood Cliffs, New Jersey, 1984.

Breiholz, D.C., 1993. "Center Core Strengthening System for Seismic Hazard Reduction of Unreinforced Masonry Bearing Wall Buildings," Structural Engineering in Natural Hazards Mitigation, Proceedings of Papers Presented at the Structures Congress '93, ASCE, Irvine, California, 1993, pp. 319-324.

Bruce, R.A., Kustu, O. and Rojahn, C., 1993. "Report and Summary of ATC-31 - Evaluation of the Performance of Seismically Retrofitted Buildings," Structural Engineering in Natural Hazards Mitigation, Proceedings of Papers Presented at the Structures Congress '93, ASCE, Irvine, California, 1993, pp. 337-342.

Bruneau, M., 1994. "State of the Art Report on Seismic Performance of Unreinforced Masonry Buildings," Journal of Structural Engineering, ASCE, New York, NY, vol. 120, no. 1, January 1994, pp. 230-259.

Campi, D.E., 1989. "Seismic Strengthening of a Historic Unreinforced Masonry Building," Seismic Engineering: Research and Practice, Proceedings of the Sessions Related to Seismic Engineering at Structures Congress '89, San Francisco, California, 1989, pp. 659-661.

Cousins, T., O'Connor, E. and Plecnik, J., 1986. "Strengthening of Unreinforced Masonry Buildings," Journal of Structural Engineering, ASCE, New York, NY, vol. 112, no. 5, May 1986, pp. 1070-1087.

Division 88: Earthquake Hazard Reduction in Existing Buildings, Los Angeles Building Code, 1985 Edition.

Green, M., 1993. "Code Provisions for URM Bearing Wall Buildings in California," Structural Engineering in Natural Hazards Mitigation, Proceedings of Papers Presented at the Structures Congress '93, ASCE, Irvine, California, 1993, pp. 313-318.

Guh, T.J. and Youssef, N., 1993. "Seismic Retrofit of Building Structures with Unreinforced Masonry Infill Walls," Structural Engineering in Natural Hazards Mitigation, Proceedings of Papers Presented at the Structures Congress '93, ASCE, Irvine, California, 1993, pp. 325-330.

Habibullah, A. and Wilson, E.L., 1990. SAP90 Users Manual - A Series of Computer Programs for the Static and Dynamic Finite Element Analysis of Structures, Computers & Structures, Inc., Berkeley, California, January 1990.

Jalil, I., Kelm, W. and Klingner, R.E., 1992. "Performance of Masonry and Masonry Veneer Buildings in the Loma Prieta Earthquake," Phil M. Ferguson Structural Engineering Laboratory Report 92-1, Department of Civil Engineering, The University of Texas at Austin, 1992.

Kariotis, J. and Nghiem, D., 1993. "In-Situ Determination of the Compressive Stress-Strain Relationship of Multi-Wythe Brick Masonry," Structural Engineering in Natural Hazards Mitigation, Proceedings of Papers Presented at the Structures Congress '93, ASCE, Irvine, California, 1993, pp. 1421-1426.

Kingsley, G.R., Kurkchubasche, A.G. and Seible, F., 1993. "Three-Dimensional Analysis Model for Complete Masonry Buildings," Structural Engineering in Natural Hazards Mitigation, Proceedings of Papers Presented at the Structures Congress '93, ASCE, Irvine, California, 1993, pp. 1185-1190.

Kosowatz, J.J., 1994. "Aid Flows to Worst U.S. Disaster," Engineering News Record, vol. 232, no. 5, January 31,1994.

Ichniowski, R. and Rosta, P., 1994. "Aid Funds Starting to Flow as Assessments Continue," Engineering News Record, vol. 232, no. 8, February 8, 1994.

McManamy, R. and Rosenbaum, D.B., 1994. "Isolating the Causes of Bad Building Behavior," Engineering News Record, vol. 232, no. 5, January 31,1994.

Mengi, Y. and McNiven, H.D., 1989. "A Mathematical Model for the In-Plane Non-Linear Earthquake Behavior of Unreinforced Masonry Walls. Part 2: Completion of the Model," Earthquake Engineering and Structural Dynamics, John Wiley & Sons, Limited, Chichester, Sussex, England, vol. 18, no. 2, February, 1989, pp. 249-261.

Tena-Colunga, A., 1992. "Seismic Evaluation of Unreinforced Masonry Structures with Flexible Diaphragms," Earthquake Spectra, Earthquake Engineering Research Institute, Berkeley, California, vol. 8, no. 2, May, 1992, pp. 305-318.

The Masonry Society, 1994. Performance of Masonry Structures in the Northridge Earthquake of January 17, 1994, Klingner, R.E., Technical Editor, The Masonry Society, Boulder, Colorado, June 1994.

Tomazevic, M., 1987. "Dynamic Modeling of Masonry Buildings: Storey Mechanism Model as a Simple Alternative," Earthquake Engineering and Structural Dynamics, John Wiley & Sons, Limited, Chichester, Sussex, England, vol. 15, no. 6, August, 1987, pp. 731-749.

VITA

Gordon Blaine Fox was born in Elmira Heights, New York on July 9, 1964, the son of Gordon and Christine Fox. After graduation from Thomas A. Edison High School in Elmira Heights, he entered West Virginia University, Morgantown, West Virginia. He completed the requirements for a Bachelor of Science Degree in Civil Engineering in December of 1986. In February, 1987, he entered Naval Officer Candidate School, Newport, Rhode Island, and was commissioned an Ensign in the United States Navy on May 29, 1987. After selection by the Navy to attend graduate school, he entered the Graduate School of the University of Texas at Austin in August, 1994 to pursue a Master of Science in Engineering Degree, with a specialization in Structural Engineering.

Permanent Address: 142 Oakwood Avenue
Elmira Heights, New York 14903

This report was typed by the author.

APPENDIX A

ANALYSIS OF 2-DIMENSIONAL VERTICAL BEAM MODEL SUBJECTED TO EARTHQUAKE LOADING

2-DIMENSIONAL VERTICAL BEAM MODEL SUBJECTED TO EARTHQUAKE LOADING

SAP90 PROGRAM OUTPUT

EIGENVALUES AND FREQUENCIES

MODE NUMBER	EIGENVALUE (RAD/SEC)**2	CIRCULAR FREQ (RAD/SEC)	FREQUENCY (CYCLES/SEC)	PERIOD (SEC)
1	.376917E+03	.194144E+02	3.089892	.323636
2	.329366E+04	.573904E+02	9.133968	.109481
3	.840500E+04	.916788E+02	14.591129	.068535
4	.213765E+05	.146207E+03	23.269567	.042975
5	.297946E+05	.172611E+03	27.471929	.036401
6	.330262E+05	.181731E+03	28.923398	.034574
7	.382923E+05	.195684E+03	31.144092	.032109
8	.681643E+05	.261083E+03	41.552652	.024066
9	.745864E+05	.273105E+03	43.466033	.023006
10	.810326E+05	.284662E+03	45.305420	.022072
11	.114798E+06	.338819E+03	53.924678	.018544
12	.116848E+06	.341830E+03	54.403880	.018381
13	.118949E+06	.344890E+03	54.890946	.018218
14	.293855E+06	.542084E+03	86.275307	.011591
15	.797737E+06	.893161E+03	142.151021	.007035
16	.151033E+07	.122896E+04	195.594491	.005113
17	.238308E+07	.154372E+04	245.691286	.004070
18	.335651E+07	.183208E+04	291.584235	.003430
19	.436427E+07	.208908E+04	332.488097	.003008
20	.533770E+07	.231035E+04	367.702995	.002720

VERTICAL BEAM SUBJECTED TO EARTHQUAKE LOADING: SAP90 DATA FILE SYSTEM
V=20 : Number of Modes Calculated in Eigenvalue Analysis
JOINTS
1 X=0 Y=0 Z=0
13 X=0 Y=0 Z=36 G=1,13,1
14 X=1 Y=0 Z=0 : Reference Node for Program

RESTRAINTS
1 R=1,1,1,1,1,1 : Freedom in the X-Z Plane Only
2,13,1 R=0,1,0,1,0,1
14 R=1,1,1,1,1,1

MASSES
5,13,4 M=2.48447,0,0,0,0,0 : Diaphragm Masses Lumped at Floor Levels

FRAME
NM=1
1 A=156 I=25073,25073 AS=50,50 E=64800 G=3512 M=0.58191: Masonry Walls
1 1 2 M=1 LP=0,14 G=11,1,1,1,0,0

TIMEH
ATYPE=0 NSTEP=1200 DT=0.02 NF=1 D=0.02 NV=20 : E-W Northridge, CA
NF=1 PRIN=1 NPL=6 DT=0.02 : Santa Monica City Hall

2.37E-03	1.68E-03	8.71E-04	-1.92E-04	-1.52E-03	-1.58E-04
1.59E-03	1.50E-03	1.50E-03	2.39E-04	-1.76E-03	-5.17E-04
3.37E-04	1.43E-05	1.05E-03	1.95E-03	1.30E-03	-1.21E-03
-4.40E-04	1.01E-03	1.74E-03	1.37E-03	-1.29E-03	-1.67E-03
-5.05E-04	3.35E-03	4.80E-03	-5.81E-05	-2.18E-03	3.16E-05
2.44E-03	4.01E-03	3.27E-03	-1.93E-03	-4.88E-03	-3.68E-04
5.06E-03	2.83E-03	-7.83E-04	-1.97E-03	-3.93E-03	-1.54E-03
4.69E-04	-7.74E-04	-3.46E-03	-1.50E-03	5.46E-03	5.09E-04
-3.25E-03	-2.05E-03	-6.48E-03	-3.33E-04	5.71E-03	-2.90E-04
-6.76E-03	-2.02E-03	3.25E-03	-3.86E-03	-5.71E-03	-3.67E-03
-3.66E-03	1.57E-03	1.71E-03	2.91E-04	-2.13E-03	-4.88E-03
4.70E-04	1.91E-03	6.21E-03	6.27E-03	-3.69E-04	-9.17E-05
8.18E-03	1.54E-02	9.72E-03	2.64E-03	-3.64E-03	-1.15E-03
3.05E-03	-5.26E-03	-1.27E-02	-9.97E-03	-5.05E-03	-5.83E-03
-9.21E-03	-8.76E-03	-7.50E-03	-5.91E-03	6.01E-04	7.08E-03
5.99E-03	1.07E-03	5.31E-03	8.03E-03	8.24E-04	-8.34E-03
-1.15E-02	-6.68E-03	-4.47E-03	-6.03E-03	-8.79E-03	-6.52E-03
4.71E-03	1.12E-02	7.89E-03	4.11E-03	7.50E-03	1.36E-02

1.45E-02	1.33E-02	1.24E-02	7.92E-03	1.82E-03	-4.80E-03
-8.80E-03	2.29E-03	1.33E-02	1.51E-02	6.01E-03	-1.44E-03
-4.62E-03	-1.29E-02	-2.46E-02	-3.00E-02	-2.47E-02	-2.34E-02
-2.93E-02	-3.16E-02	-3.27E-02	-4.17E-02	-4.25E-02	-2.92E-02
-1.32E-02	-6.42E-03	-1.01E-02	-1.83E-02	-2.80E-02	-2.95E-02
-2.30E-02	-1.19E-02	1.75E-04	1.21E-02	2.22E-02	2.50E-02
1.43E-02	-2.55E-03	-1.75E-02	-1.74E-02	-5.90E-03	9.73E-03
2.57E-02	3.55E-02	3.49E-02	2.41E-02	1.46E-02	1.23E-02
1.53E-02	1.99E-02	2.47E-02	2.35E-02	2.00E-02	2.23E-02
2.20E-02	1.62E-02	1.14E-02	1.69E-02	3.01E-02	3.90E-02
3.47E-02	2.40E-02	1.80E-02	1.32E-02	1.44E-02	2.21E-02
2.89E-02	2.58E-02	1.65E-02	9.22E-03	3.72E-03	-1.45E-03
-7.99E-03	-1.20E-02	-1.37E-02	-1.18E-02	-5.62E-03	1.44E-04
4.65E-03	8.24E-03	1.15E-02	1.38E-02	1.15E-02	8.56E-03
8.11E-03	1.22E-02	1.68E-02	1.18E-02	3.48E-03	-5.78E-03
-1.02E-02	-8.26E-03	-3.24E-03	1.09E-03	8.50E-04	-3.23E-03
-9.65E-03	-9.44E-03	-6.39E-03	-6.71E-03	-1.21E-02	-1.81E-02
-2.28E-02	-2.86E-02	-2.93E-02	-2.26E-02	-1.46E-02	-1.23E-02
-1.57E-02	-1.74E-02	-1.94E-02	-2.18E-02	-2.25E-02	-2.26E-02
-1.86E-02	-1.11E-02	-2.96E-03	-3.44E-04	-1.65E-03	-4.06E-04
1.41E-03	-3.13E-03	-5.75E-03	2.99E-04	4.78E-03	4.11E-03
-5.23E-03	-1.85E-02	-2.70E-02	-2.43E-02	-1.61E-02	-1.17E-02
-1.15E-02	-1.14E-02	-1.52E-02	-2.13E-02	-2.19E-02	-1.96E-02
-1.61E-02	-1.64E-02	-1.55E-02	-1.23E-02	-7.02E-03	1.77E-03
7.59E-03	6.22E-03	1.84E-03	1.79E-03	3.95E-03	6.31E-03
5.40E-03	9.28E-03	1.72E-02	2.18E-02	2.08E-02	2.02E-02
2.63E-02	3.21E-02	3.34E-02	2.83E-02	2.15E-02	1.68E-02
1.87E-02	2.69E-02	3.71E-02	4.42E-02	4.70E-02	4.54E-02
4.01E-02	3.32E-02	2.42E-02	1.25E-02	1.05E-03	-6.77E-03
-5.76E-03	7.67E-04	5.45E-03	5.07E-03	3.13E-03	3.14E-03
6.58E-03	1.04E-02	8.78E-03	2.88E-03	-8.12E-03	-1.74E-02
-2.14E-02	-2.37E-02	-2.49E-02	-2.26E-02	-1.82E-02	-1.56E-02
-1.42E-02	-1.31E-02	-9.04E-03	-4.34E-03	7.14E-04	4.41E-03
1.34E-03	-3.26E-03	-4.62E-03	-5.39E-03	-9.89E-03	-1.58E-02
-1.51E-02	-9.21E-03	-8.54E-03	-1.17E-02	-8.77E-03	2.09E-03
1.15E-02	1.26E-02	9.75E-03	6.60E-03	5.74E-03	7.79E-03
9.11E-03	4.13E-03	-3.32E-03	-1.00E-02	-1.48E-02	-1.77E-02
-1.90E-02	-1.60E-02	-1.29E-02	-1.30E-02	-1.52E-02	-1.28E-02
-9.35E-03	-1.02E-02	-1.12E-02	-1.07E-02	-9.17E-03	-5.35E-03
-3.06E-03	-2.18E-03	1.71E-03	5.18E-03	4.05E-03	-3.07E-03
-5.25E-03	7.32E-04	3.84E-03	5.11E-03	5.35E-03	2.25E-03
-1.69E-03	-4.07E-03	-2.64E-03	2.41E-03	3.15E-03	-3.07E-03
-8.85E-03	-9.60E-03	-4.71E-03	1.04E-04	3.59E-03	3.62E-03

LC=-1 NF=1 S=32.17 ANGLE=0.0 AT=0.0

APPENDIX B

ANALYSIS OF 3-DIMENSIONAL FINITE ELEMENT MODEL OF PROTOTYPE URM BUILDING

3-DIMENSIONAL FINITE ELEMENT MODEL OF PROTOTYPE URM BUILDING SUBJECTED TO EARTHQUAKE LOADING

SAP90 PROGRAM OUTPUT

EIGENVALUES AND FREQUENCIES

MODE NUMBER	EIGENVALUE (RAD/SEC)**2	CIRCULAR FREQ (RAD/SEC)	FREQUENCY (CYCLES/SEC)	PERIOD (SEC)
1	.228470E+03	.151152E+02	2.405664	.415686
2	.241922E+03	.155539E+02	2.475473	.403963
3	.246621E+03	.157042E+02	2.499398	.400096
4	.443799E+03	.210665E+02	3.352843	.298254
5	.116535E+04	.341373E+02	5.433115	.184056
6	.125828E+04	.354723E+02	5.645590	.177129
7	.130785E+04	.361643E+02	5.755723	.173740
8	.317348E+04	.563336E+02	8.965777	.111535
9	.345239E+04	.587570E+02	9.351475	.106935
10	.356536E+04	.597107E+02	9.503249	.105227
11	.365630E+04	.604674E+02	9.623682	.103910
12	.710553E+04	.842943E+02	13.415856	.074539
13	.753511E+04	.868050E+02	13.815451	.072383
14	.873293E+04	.934502E+02	14.873054	.067236
15	.105657E+05	.102790E+03	16.359494	.061127
16	.117801E+05	.108536E+03	17.274074	.057890
17	.131835E+05	.114819E+03	18.274049	.054722
18	.145750E+05	.120727E+03	19.214284	.052045
19	.147219E+05	.121334E+03	19.310895	.051784
20	.149128E+05	.122118E+03	19.435665	.051452

SAP90 PROGRAM OUTPUT

MODE SHAPE NUMBER 4
PERIOD = .298254 SECONDS

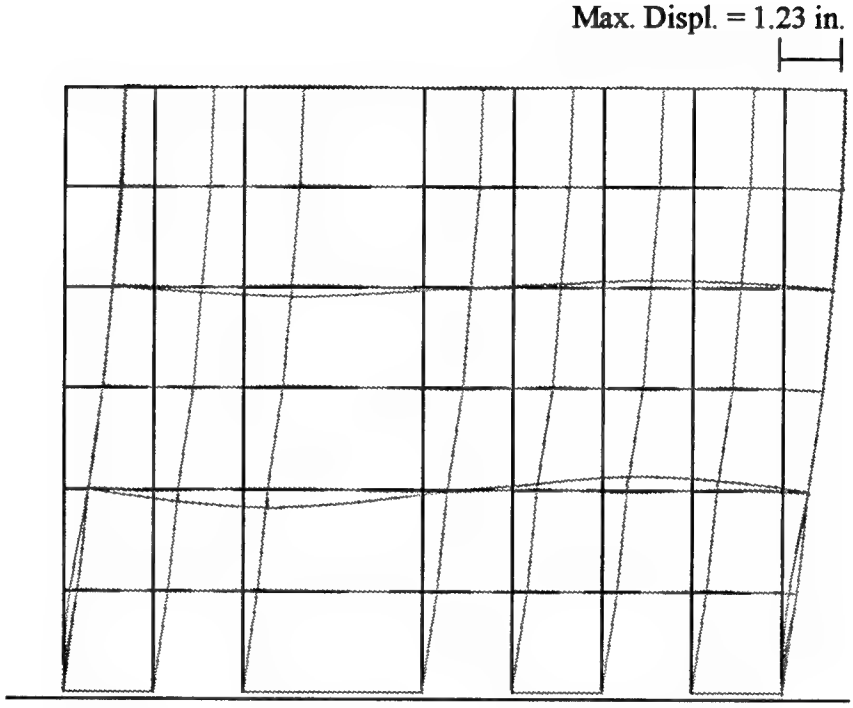

Figure B-1: Fourth Deformed Mode Shape for 3-D Model

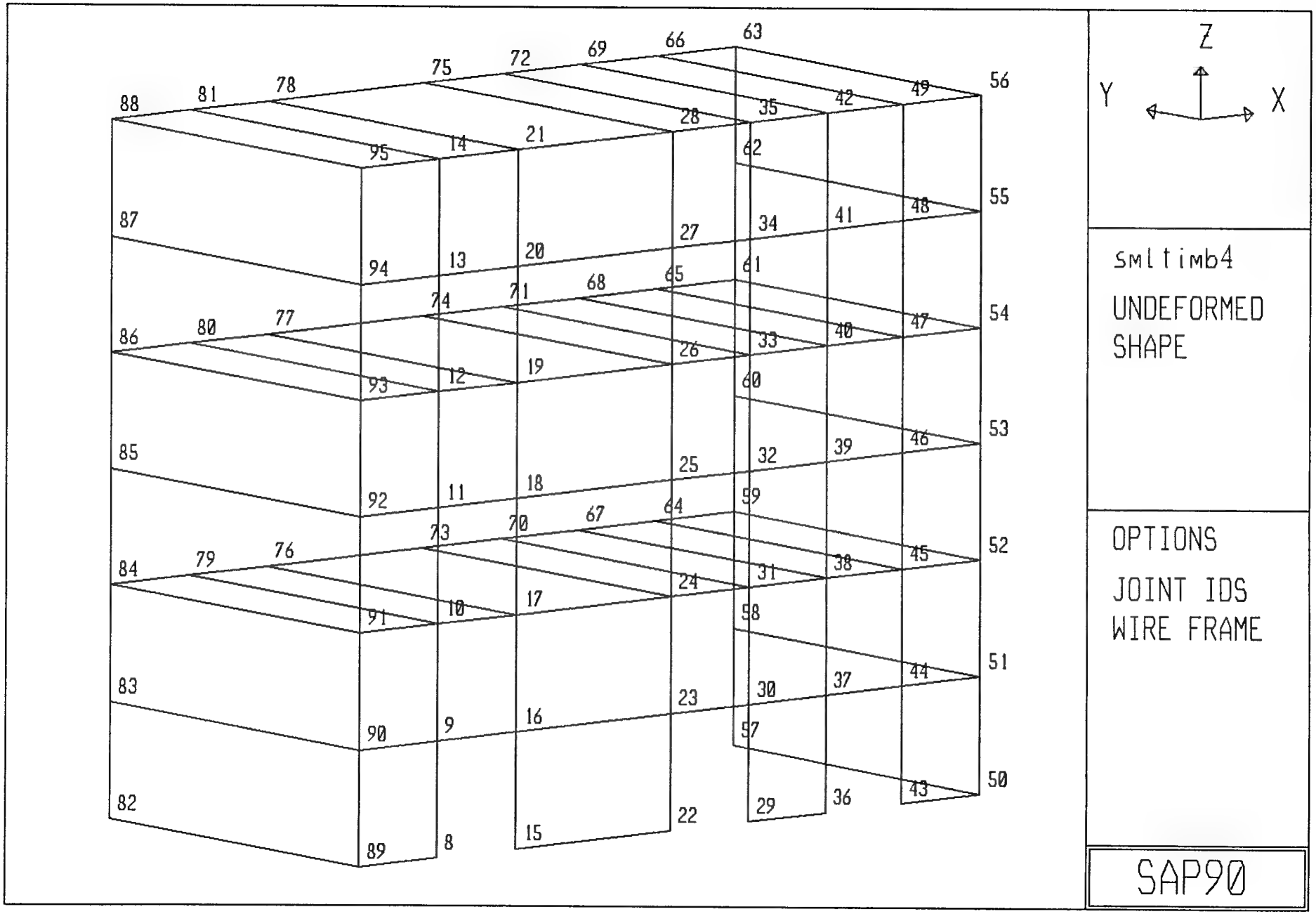

Figure B-2: Finite Element Mesh for 3 Dimensional Model

```
THREE STORY UNREINFORCED MASONRY (URM) BUILDING:  SAP90 DATA
SYSTEM
V=20          : Number of Modes to be Calculated in Eigenvalue Analysis
JOINTS
1       X=0     Y=0     Z=0
7       X=0     Y=0     Z=36    G=1,7,1
15      X=10    Y=0     Z=0
21      X=10    Y=0     Z=36    Q=1,7,15,21,1,7
22      X=20    Y=0     Z=0
28      X=20    Y=0     Z=36    G=22,28,1
50      X=40    Y=0     Z=0
56      X=40    Y=0     Z=36    Q=22,28,50,56,1,7
57      X=40    Y=20    Z=0
63      X=40    Y=20    Z=36    G=57,63,1
64      X=35    Y=20    Z=12
66      X=35    Y=20    Z=36
73      X=20    Y=20    Z=12
75      X=20    Y=20    Z=36    Q=64,66,73,75,1,3
76      X=10    Y=20    Z=12
78      X=10    Y=20    Z=36
79      X=5     Y=20    Z=12
81      X=5     Y=20    Z=36    Q=76,78,79,81,1,3
82      X=0     Y=20    Z=0
88      X=0     Y=20    Z=36    G=82,88,1
89      X=0     Y=0     Z=0
95      X=0     Y=0     Z=36    G=89,95,1

RESTRAINTS
57  88  1   R=0,1,0,1,0,1
1   57  7   R=1,1,1,1,1,1
82  89  7   R=1,1,1,1,1,1

SHELL
NM=2
1   E=64800      U=0.2     M=0.12/32.2    : Masonry Properties using Kips and Feet
2   E=150000     U=0.2     M=0.10/32.2  :  Wood        "       "       "       "       "
34  JQ=  50, 51,  57,  58   M=1  ETYPE=0  TH=1  G=6,1: Masonry Out-of-
Plane Walls
40  JQ=  82, 83,  89,  90   M=1  ETYPE=0  TH=1  G=6,1
46  JQ=  91, 10,  84,  79   M=2  ETYPE=0  TH=0.5:        Timber Diaphragms
47  JQ=  10, 17,  79,  76   M=2  ETYPE=0  TH=0.5
48  JQ=  17, 24,  76,  73   M=2  ETYPE=0  TH=0.5
49  JQ=  24, 31,  73,  70   M=2  ETYPE=0  TH=0.5
```

```
50  JQ=  31, 38,  70,  67  M=2  ETYPE=0  TH=0.5
51  JQ=  38, 45,  67,  64  M=2  ETYPE=0  TH=0.5
52  JQ=  45, 52,  64 , 59  M=2  ETYPE=0  TH=0.5
53  JQ=  93, 12,  86,  80  M=2  ETYPE=0  TH=0.5
54  JQ=  12, 19,  80,  77  M=2  ETYPE=0  TH=0.5
55  JQ=  19, 26,  77,  74  M=2  ETYPE=0  TH=0.5
56  JQ=  26, 33,  74,  71  M=2  ETYPE=0  TH=0.5
57  JQ=  33, 40,  71,  68  M=2  ETYPE=0  TH=0.5
58  JQ=  40, 47,  68,  65  M=2  ETYPE=0  TH=0.5
59  JQ=  47, 54,  65,  61  M=2  ETYPE=0  TH=0.5
60  JQ=  95, 14,  88,  81  M=2  ETYPE=0  TH=0.5
61  JQ=  14, 21,  81,  78  M=2  ETYPE=0  TH=0.5
62  JQ=  21, 28,  78,  75  M=2  ETYPE=0  TH=0.5
63  JQ=  28, 35,  75,  72  M=2  ETYPE=0  TH=0.5
64  JQ=  35, 42,  72,  69  M=2  ETYPE=0  TH=0.5
65  JQ=  42, 49,  69,  66  M=2  ETYPE=0  TH=0.5
66  JQ=  49, 56,  66,  63  M=2  ETYPE=0  TH=0.5

ASOLID
NM=1     ETYPE=2     MAXN=1
1        NUMT=1      M=0.12/32.2 :              Masonry Shear Walls
T=0      E=64800,64800   U=0.2,0.2  G=3512
1   JQ=   89, 90,   8,   9  M=1    TH=1  G=6,1  LP=3
7   JQ=    9,  10,  16,  17  M=1    TH=1  LP=3
8   JQ=   11,  12,  18,  19  M=1    TH=1  LP=3
9   JQ=   13,  14,  20,  21  M=1    TH=1  LP=3
10  JQ=   15,  16,  22,  23  M=1    TH=1  G=6,1  LP=3
16  JQ=   23,  24,  30,  31  M=1    TH=1  LP=3
17  JQ=   25,  26,  32,  33  M=1    TH=1  LP=3
18  JQ=   27,  28,  34,  35  M=1    TH=1  LP=3
19  JQ=   29,  30,  36,  37  M=1    TH=1  G=6,1  LP=3
25  JQ=   37,  38,  44,  45  M=1    TH=1  LP=3
26  JQ=   39,  40,  46,  47  M=1    TH=1  LP=3
27  JQ=   41,  42,  48,  49  M=1    TH=1  LP=3
28  JQ=   43,  44,  50,  51  M=1    TH=1  G=6,1  LP=3

TIMEH
ATYPE=0    NSTEP=1200   DT=0.02   NF=1     D=0.02     NV=20
NF=1       PRIN=1       NPL=6     DT=0.02
 2.37E-03    1.68E-03    8.71E-04   -1.92E-04   -1.52E-03   -1.58E-04
 1.59E-03    1.50E-03    1.50E-03    2.39E-04   -1.76E-03   -5.17E-04
 3.37E-04    1.43E-05    1.05E-03    1.95E-03    1.30E-03   -1.21E-03
-4.40E-04    1.01E-03    1.74E-03    1.37E-03   -1.29E-03   -1.67E-03
-5.05E-04    3.35E-03    4.80E-03   -5.81E-05   -2.18E-03    3.16E-05
```

2.44E-03	4.01E-03	3.27E-03	-1.93E-03	-4.88E-03	-3.68E-04
5.06E-03	2.83E-03	-7.83E-04	-1.97E-03	-3.93E-03	-1.54E-03
4.69E-04	-7.74E-04	-3.46E-03	-1.50E-03	5.46E-03	5.09E-04
-3.25E-03	-2.05E-03	-6.48E-03	-3.33E-04	5.71E-03	-2.90E-04
-6.76E-03	-2.02E-03	3.25E-03	-3.86E-03	-5.71E-03	-3.67E-03
-3.66E-03	1.57E-03	1.71E-03	2.91E-04	-2.13E-03	-4.88E-03
4.70E-04	1.91E-03	6.21E-03	6.27E-03	-3.69E-04	-9.17E-05
8.18E-03	1.54E-02	9.72E-03	2.64E-03	-3.64E-03	-1.15E-03
3.05E-03	-5.26E-03	-1.27E-02	-9.97E-03	-5.05E-03	-5.83E-03
-9.21E-03	-8.76E-03	-7.50E-03	-5.91E-03	6.01E-04	7.08E-03
5.99E-03	1.07E-03	5.31E-03	8.03E-03	8.24E-04	-8.34E-03
-1.15E-02	-6.68E-03	-4.47E-03	-6.03E-03	-8.79E-03	-6.52E-03
4.71E-03	1.12E-02	7.89E-03	4.11E-03	7.50E-03	1.36E-02
1.45E-02	1.33E-02	1.24E-02	7.92E-03	1.82E-03	-4.80E-03
-8.80E-03	2.29E-03	1.33E-02	1.51E-02	6.01E-03	-1.44E-03
-4.62E-03	-1.29E-02	-2.46E-02	-3.00E-02	-2.47E-02	-2.34E-02
-2.93E-02	-3.16E-02	-3.27E-02	-4.17E-02	-4.25E-02	-2.92E-02
-1.32E-02	-6.42E-03	-1.01E-02	-1.83E-02	-2.80E-02	-2.95E-02
-2.30E-02	-1.19E-02	1.75E-04	1.21E-02	2.22E-02	2.50E-02
1.43E-02	-2.55E-03	-1.75E-02	-1.74E-02	-5.90E-03	9.73E-03
2.57E-02	3.55E-02	3.49E-02	2.41E-02	1.46E-02	1.23E-02
1.53E-02	1.99E-02	2.47E-02	2.35E-02	2.00E-02	2.23E-02
2.20E-02	1.62E-02	1.14E-02	1.69E-02	3.01E-02	3.90E-02
3.47E-02	2.40E-02	1.80E-02	1.32E-02	1.44E-02	2.21E-02
2.89E-02	2.58E-02	1.65E-02	9.22E-03	3.72E-03	-1.45E-03
-7.99E-03	-1.20E-02	-1.37E-02	-1.18E-02	-5.62E-03	1.44E-04
4.65E-03	8.24E-03	1.15E-02	1.38E-02	1.15E-02	8.56E-03
8.11E-03	1.22E-02	1.68E-02	1.18E-02	3.48E-03	-5.78E-03
-1.02E-02	-8.26E-03	-3.24E-03	1.09E-03	8.50E-04	-3.23E-03
-9.65E-03	-9.44E-03	-6.39E-03	-6.71E-03	-1.21E-02	-1.81E-02
-2.28E-02	-2.86E-02	-2.93E-02	-2.26E-02	-1.46E-02	-1.23E-02
-1.57E-02	-1.74E-02	-1.94E-02	-2.18E-02	-2.25E-02	-2.26E-02
-1.86E-02	-1.11E-02	-2.96E-03	-3.44E-04	-1.65E-03	-4.06E-04
1.41E-03	-3.13E-03	-5.75E-03	2.99E-04	4.78E-03	4.11E-03
-5.23E-03	-1.85E-02	-2.70E-02	-2.43E-02	-1.61E-02	-1.17E-02
-1.15E-02	-1.14E-02	-1.52E-02	-2.13E-02	-2.19E-02	-1.96E-02
-1.61E-02	-1.64E-02	-1.55E-02	-1.23E-02	-7.02E-03	1.77E-03
7.59E-03	6.22E-03	1.84E-03	1.79E-03	3.95E-03	6.31E-03
5.40E-03	9.28E-03	1.72E-02	2.18E-02	2.08E-02	2.02E-02
2.63E-02	3.21E-02	3.34E-02	2.83E-02	2.15E-02	1.68E-02
1.87E-02	2.69E-02	3.71E-02	4.42E-02	4.70E-02	4.54E-02
4.01E-02	3.32E-02	2.42E-02	1.25E-02	1.05E-03	-6.77E-03
-5.76E-03	7.67E-04	5.45E-03	5.07E-03	3.13E-03	3.14E-03
6.58E-03	1.04E-02	8.78E-03	2.88E-03	-8.12E-03	-1.74E-02

(not complete record)

-2.14E-02	-2.37E-02	-2.49E-02	-2.26E-02	-1.82E-02	-1.56E-02
-1.42E-02	-1.31E-02	-9.04E-03	-4.34E-03	7.14E-04	4.41E-03
1.34E-03	-3.26E-03	-4.62E-03	-5.39E-03	-9.89E-03	-1.58E-02
-1.51E-02	-9.21E-03	-8.54E-03	-1.17E-02	-8.77E-03	2.09E-03
1.15E-02	1.26E-02	9.75E-03	6.60E-03	5.74E-03	7.79E-03
9.11E-03	4.13E-03	-3.32E-03	-1.00E-02	-1.48E-02	-1.77E-02
-1.90E-02	-1.60E-02	-1.29E-02	-1.30E-02	-1.52E-02	-1.28E-02
-9.35E-03	-1.02E-02	-1.12E-02	-1.07E-02	-9.17E-03	-5.35E-03
-3.06E-03	-2.18E-03	1.71E-03	5.18E-03	4.05E-03	-3.07E-03
-5.25E-03	7.32E-04	3.84E-03	5.11E-03	5.35E-03	2.25E-03
-1.69E-03	-4.07E-03	-2.64E-03	2.41E-03	3.15E-03	-3.07E-03
-8.85E-03	-9.60E-03	-4.71E-03	1.04E-04	3.59E-03	3.62E-03

LC=-1 NF=1 S=32.17 ANGLE=0.0 AT=0.0